Journal of Thermal Analysis and Calorimetry (2019) 138:3229–3248
https://doi.org/10.1007/s10973-019-08610-0

Handling complexity in biological interactions

Allostery and cooperativity in proteins

Sonia Vega[1] · Olga Abian[1,2,3,4,5] · Adrian Velazquez-Campoy[1,2,3,4,6]

Received: 11 March 2019 / Accepted: 19 July 2019 / Published online: 10 August 2019

Abstract
Biological processes rely on interactions between many binding partners. Binding results in the modulation of the conformational landscape of the interacting molecules, a phenomenon rooted in folding and binding cooperativity underlying the allosteric functional regulation of biomacromolecules. The conformational equilibrium of a protein and the binding equilibria of different interacting and cooperative ligands are coupled giving rise to a complex scenario in which protein function can be finely tuned and modulated. Binding cooperativity and allostery add additional levels of complexity in protein function regulation. Here we will review some important concepts associated with binding, cooperativity and allostery in protein interactions, illustrated with several representative protein-dependent biological systems related to drug discovery and physiological mechanisms characterization and studied by isothermal titration calorimetry.

Keywords Allostery · Interaction cooperativity · Ligand binding · Binding polynomial · Conformational landscape · Biochemical linkage

Introduction

> Misura ciò che è misurabile, e rendi misurabile ciò che non lo è
> Galileo Galilei, 1564–1642

Biological processes can be rationalized on the basis of multiple interactions between many binding partners. They involve the interplay of multiple interacting agents; in particular, proteins show complex conformational equilibria, and at the same time, they are able to bind different small and large biomolecules as ligands. Thus, very often ligand binding results in the modulation of the conformational landscape (ensemble of conformational states and their populations) of the protein, a phenomenon rooted in folding and binding cooperativity, which is macroscopically observed as ligand-induced conformational changes.

The ligand-dependent conformational equilibrium of a protein represent the structural and energetic basis of allostery, a phenomenon underlying protein activity regulation. The preexisting conformational equilibrium between different conformational protein states and their different ligand binding capabilities represents the basic elements for the allosteric regulation that explains the finely tuned biological response (protein activity or function) as a function of the biochemical input (concentration of ligand: substrate, cofactor, inhibitor, activator).

A large percentage of the interactions studied in the laboratory correspond to a simple 1:1 interaction. In

✉ Olga Abian
oabifra@unizar.es

✉ Adrian Velazquez-Campoy
adrianvc@unizar.es

[1] Institute of Biocomputation and Physics of Complex Systems (BIFI), Joint Units IQFR-CSIC-BIFI, and GBsC-CSIC-BIFI, Universidad de Zaragoza, 50018 Zaragoza, Spain

[2] Departamento de Bioquímica y Biología Molecular y Celular, Universidad de Zaragoza, 50009 Zaragoza, Spain

[3] Aragon Institute for Health Research (IIS Aragon), 50009 Zaragoza, Spain

[4] Biomedical Research Networking Centre for Liver and Digestive Diseases (CIBERehd), Madrid, Spain

[5] Aragon Health Sciences Institute (IACS), 50009 Zaragoza, Spain

[6] ARAID Foundation, Government of Aragon, 50018 Zaragoza, Spain

addition, very often the influence of additional ligands on a given interaction can be considered implicitly through apparent binding parameters, and linkage relationships can be employed for extracting invaluable information. However, there are some situations where complexity cannot be avoided: (1) when binding cooperativity parameters are to be quantified in a rigorous manner and (2) when the protein possesses more than one ligand binding site.

Then, how is it possible to deal with such complexity? The researcher must bear in mind important issues: (1) Which physical model would be considered? (2) Which experimental technique(s) will be employed? (3) Which experimental setup would be designed and implemented? (4) What information would be required prior to the experimental work and data analysis? (5) What information experimentally accessible would be available after the experiments? and (6) Which are the limitations of the model and the experimental techniques employed?

The general allosteric model is the appropriate conceptual and operational tool for handling simultaneously conformational variability and ligand binding capability [1]. Together with the formalism of the binding polynomial or binding partition function [2–4], it is possible to study virtually any biological system: not only allosteric systems, but also polysteric systems.

Here we will review some important concepts associated with binding, cooperativity and allostery in protein interactions, illustrated with several representative protein-dependent biological systems studied experimentally by isothermal titration calorimetry. Although the analysis of ITC experiments can be performed even without applying nonlinear least squares fitting analysis, by relying on the geometric features of the binding isotherm [5], the only way to rigorously extract precise and valuable information on complex interactions requires application of appropriate models based on the binding polynomial, making use of mass conservation and chemical equilibrium equations. A detailed explanation of the application of the binding polynomial and its application to ITC experiments can be found elsewhere [6–8].

Cooperativity and allostery

Christian Bohr [9] reported the influence of carbon dioxide concentration and pH on the ability of hemoglobin to bind oxygen much earlier than the structural details on this protein were elucidated. The interplay of oxygen, carbon dioxide and free protons represents the prototypical example of cooperative binding effects for which Wyman coined much later the terms "homotropic" and "heterotropic" cooperativity: The binding of a ligand is affected by the binding of the same or a different ligand [4].

Additional evidences from other biological systems led to establishing the concept of "allostery" and "allosteric control", intimately connected to cooperativity, in which ligand binding is coupled to a preexisting equilibrium between different protein conformations exhibiting different ligand binding affinities and activities [10, 11]. Ligand binding shifts the populations of the protein states through conformational transitions ("allosteric transitions") governed by ligand affinity and regulates protein function by conditioning further interactions. That way the binding of a ligand may influence the binding of a subsequent ligand.

The phenomenological definition of allostery is the control or modulation of the ligand binding equilibrium by the binding of another ligand. In other words, the binding of a ligand to a given site in a protein can be affected by the occupation of another site by another ligand. However, that simplistic interpretation sheds no light on a plausible mechanism for allostery, and it may be erroneously concluded that just mere ligand–protein collisions may be the cause of regulatory protein conformational changes.

The original mechanistic definition of allostery, very often overlooked nowadays, is the control or modulation of the protein conformational equilibrium by the binding of a ligand. The binding of a ligand to a given site in a protein can affect the conformational equilibrium of the protein. This conformational equilibrium controlled by ligand binding will affect any additional ligand binding event because the different conformational states within the protein conformational landscape display different structural and functional properties.

The protein conformational landscape

It is currently assumed that the conformational landscape of a protein contains not only the native, folded and structured macrostate (an ensemble of closely structurally and functionally related conformational microstates) with the lowest Gibbs energy under native conditions, but also the unfolded and unstructured macrostate with much higher Gibbs energy, and a vast diversity of partially unfolded states, many of them with intermediate Gibbs energies between those of the native and the unfolded states, and many of them with Gibbs energies much higher than that of the unfolded macrostate. This complex conformational landscape may be conditioned by the existence of structural or energetic domains within the protein molecule, which will restrict the conformational landscape from a practical point of view to a set of discrete and distinguishable conformational macrostates in which those domains are either fully structured or fully unstructured in a quasi-independent fashion. In addition, this conformational landscape may be controlled or modulated by ligand binding. The

relevant conformational states will be those showing intermediate energies between those of the native state and the completely unfolded state. In general, the conformational landscape of a protein can be represented by a set of many states characterized by their conformation and their complexation with ligands. However, all those states can be clustered according to structural and/or functional similarities. For the rest of this work, we will consider a discrete conformational landscape consisting of a set of structurally and functionally distinguishable and relevant macrostates, regarding conformation or ligand complexation; each macrostate consists of a subensemble or cluster of structurally and functionally similar microstates (Fig. 1).

The population or the molar fraction of a given conformational state depends on its Gibbs energy: The lower its Gibbs energy, the larger its population, according to the Maxwell–Boltzmann statistics. Ligand binding to a given conformational state stabilizes and increases the population of that state by reducing its overall (conformational plus binding) Gibbs energy. As a result of the ligand interaction, all states within the conformational landscape will undergo a population change or shift, even for those states not interacting with the ligand, because populations are dependent on relative differences in Gibbs energies, not absolute Gibbs energies. Some states will increase their population (those preferentially interacting with the ligand), and some of them will decrease their population (those not interacting with the ligand). And therefore, ligand-induced conformational changes are the macroscopic manifestations of ligand-induced population shifts in the preexisting conformational equilibrium, not the results or "side effects" of protein–ligand collisions. Because each conformational state may exhibit different functional properties (e.g., binding a given partner or certain enzymatic activity), the predominant states in the conformational landscape of a protein determine the functional properties of the protein. Thus, summarizing, the interaction with a certain ligand: (1) alters the protein conformational landscape by modifying the population of the different states and (2) modulates the protein function by determining further interactions with other biomolecules (Fig. 1).

From the previous discussion, it can be concluded that: (1) all proteins are allosteric, since all proteins show a conformational equilibrium controlled by ligand binding, and ligand binding is further influenced by the binding of additional ligands [1, 12]; and (2) all proteins exhibit homotropic and heterotropic cooperativity, since any protein is able to interact with more than one ligand. The basic example for these statements is the pH dependence of the structural stability, the ligand binding affinity or the activity in proteins as a result of the coupling with proton association/dissociation equilibria. In addition, cooperativity and allostery do not require quaternary structure or molecular symmetry, because monomeric non-symmetric proteins may display cooperativity and allostery.

Although cooperativity and allostery are deeply interconnected, from a rigorous point of view they are not fully reciprocal: A protein exhibiting binding cooperativity is

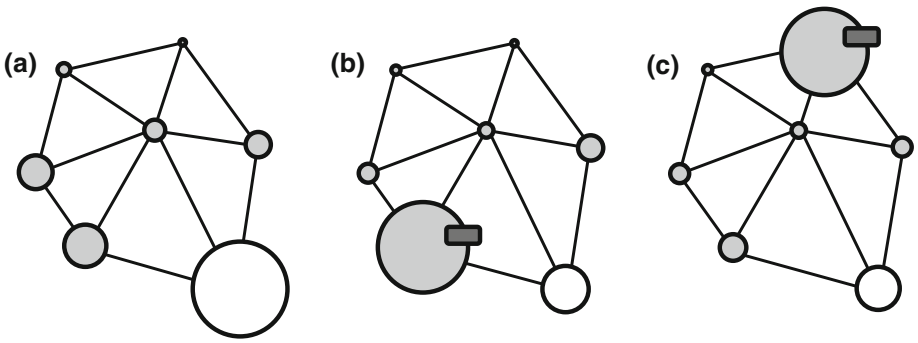

Fig. 1 Schematic representation of the conformational landscape of a protein. Each circle represents a distinguishable conformational macrostate, which is an ensemble of closely similar conformational and functional microstates. The size of the circle is a measure of the population, the molar fraction or the statistical mass of that state within the full landscape. The lines connecting states represent potential conformational transitions between different conformational states. The most populated states dominate the landscape, and their functional properties dominate the observed functional characteristics of the protein under certain conditions. Different factors (e.g., temperature, pressure, ionic concentrations, presence of ligands and mutations in the protein) can alter the conformational landscape by modifying the population distribution of the conformational states. Among those factors, ligand binding is one of the most determinant factors in vivo. Given a conformational landscape dominated by a certain conformational state (white circle) under certain circumstances (**a**), if a ligand (dark gray rectangle) is present, it may bind to the most populated state, further stabilizing it and, therefore, not exerting a significant alteration in the conformational landscape. But, if the ligand binds to a less populated state (**b**) or to a negligibly populated state (**c**) and stabilize it, that conformational state will now be the predominant state governing the biological response (protein function or activity). The extent of the stabilization and the concomitant increase in the population for each state depends on the ligand binding affinity, the ligand binding stoichiometry and the concentration of ligand. Being ligand binding affinity and stoichiometry intrinsic properties for each protein conformational state, the nature of the ligand and its concentration is the biochemical input resulting in a different biological response under certain circumstances

allosteric, but an allosteric protein does not necessarily exhibit binding cooperativity. A minimal monomeric protein with a single binding site for a ligand and displaying two conformational states, one of them able to interact with the ligand, is an allosteric, because ligand binding will shift the conformational landscape toward the binding-competent state, but it is not cooperative, since a single ligand binding site cannot show cooperativity. The same occurs if the two allosterically related conformational states are able to bind the ligand, but one state shows higher affinity. Importantly, because the two conformational states are in equilibrium and they interconvert between each other, the overall behavior is that of a protein with a single binding site with apparent ensemble-averaged binding parameters, no matter how large the extension of the conformational change linking both conformational states is [7, 13].

Structural similarity or homology in proteins or ligands does not result in similar behavior regarding binding affinity, allostery or binding cooperativity. For example, it is known that: (1) similar ligands bind to a given protein with different binding affinities and/or different cooperativity effects [14, 15]; (2) similar proteins bind the same ligand with different binding affinities and/or different cooperativity effects [16]; and (3) similar proteins exhibit markedly different conformational landscapes and different susceptibilities for the same ligand [17–19].

The general allosteric model: conformational and ligand binding equilibria

Wyman realized the behavior of proteins interacting with ligands could be modeled in a very general way through the use of the general allosteric model and the binding polynomial. Starting from them, key features, such as the linkage relationships, can be outlined [4, 20, 21].

The general allosteric model is the formal representation of the conformational landscape and its coupling with ligand binding (Fig. 2). This model considers a variety of conformational states P_s that are able to bind up to n molecules of ligand A. Then, the binding polynomial, Z, for the system is expressed as the relative fraction of all macromolecular species taking as a reference the unliganded, native state P_0:

$$Z = \sum_{s=0}^{t}\sum_{i=0}^{n}\frac{[P_sA_i]}{[P_0]} = \sum_{s=0}^{t}\sum_{i=0}^{n}\frac{\beta_{si}[P_s][A]^i}{[P_0]} = \sum_{s=0}^{t}\sum_{i=0}^{n}\beta_{si}\gamma_s[A]^i \quad (1)$$

where P_sA_i represents the complex between the protein in conformational state s with i ligand A molecules bound and β_{si} is its corresponding overall stoichiometric association constant (that is, it represents an ensemble of different complexes sharing the same conformational state and the same number of ligand A molecules bound, but with potentially many different internal configurations regarding the location of the ligand A molecules within the macromolecule), and γ_s is the conformational equilibrium constant for the conformational state s (with $\gamma_0 = 1$). The fraction or population of each protein species in equilibrium is expressed as:

$$\chi_{si} = \frac{[P_sA_i]}{[P]_T} = \frac{\beta_{si}\gamma_s[A]^i}{Z} \quad (2)$$

and the main averages can be calculated directly or through the first derivatives of the partition function:

$$\begin{aligned}\langle\Delta G\rangle &= -RT\ln Z\\ n_{LB,A} &= \sum_{s=0}^{t}\sum_{i=0}^{n} i\chi_{si} = \left(\frac{\partial \ln Z}{\partial \ln[A]}\right)_{T,p...}\\ \langle\Delta H\rangle &= \sum_{s=0}^{t}\sum_{i=0}^{n}\Delta H_{si}\chi_{si} = RT^2\left(\frac{\partial \ln Z}{\partial T}\right)_{p,[A]...}\end{aligned} \quad (3)$$

where $\langle\Delta G\rangle$ is the excess average Gibbs energy of the system containing specifically the contribution of ligand A binding, $n_{LB,A}$ is the average number of ligand A molecules bound per protein molecule, T is the absolute temperature, p is the pressure, ΔH_{si} is the overall binding enthalpy associated with the formation of complex P_sA_i and $\langle\Delta H\rangle$ is the excess average binding enthalpy of the system.

It can be demonstrated (see "Appendix") that the overall stoichiometric association constants β_{si}'s can be expressed as a function of the total number of binding sites, n, the number of ligand A molecules bound per macromolecule, i, the first stoichiometric association constant for ligand A, β_{s1} (or the intrinsic site-specific association constant, K), and the cooperativity constant accounting for homotropic cooperativity effects for ligand A binding, α_{si} (with $\alpha_{s1} = 1$ for all s; that is, there is no homotropic effect for the first ligand bound):

$$\beta_{si} = \binom{n}{i} n^{-i}\beta_{s1}^{i}\alpha_{si} \quad (4)$$

The binding equations are obtained when considering the chemical equilibrium (basically, the binding polynomial) together with the mass conservation principle:

$$\begin{aligned}[A]_T &= [A] + [P]_T n_{LB,A} = [A] + [P]_T\frac{\partial \ln Z}{\partial \ln[A]}\\ [P]_T &= [P]Z\end{aligned} \quad (5)$$

and the calorimetric equation provides the heat effect, q, per individual injection k (binding isotherm) when injecting ligand A into protein P:

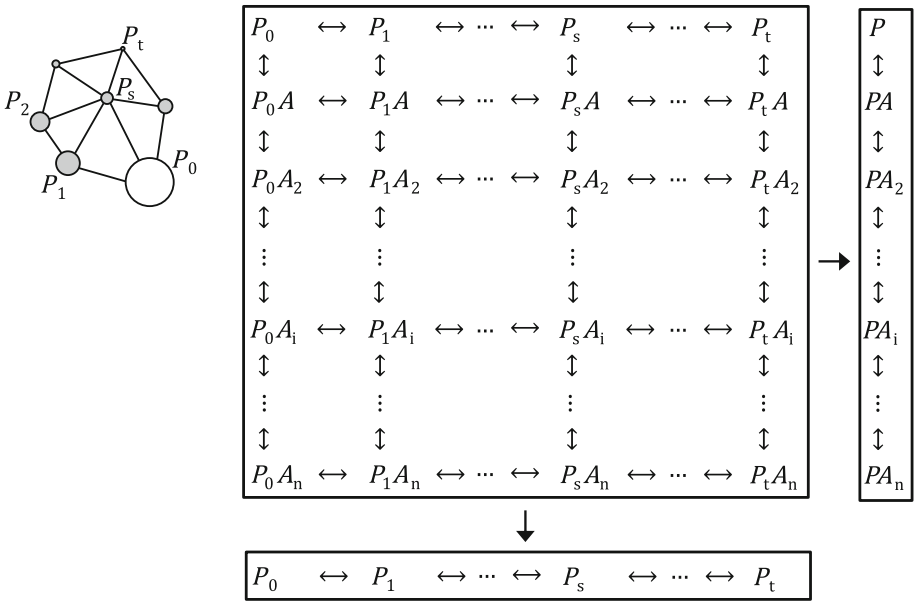

Fig. 2 Chart corresponding to the general allosteric model for the coupling of conformational equilibrium and ligand binding (homotropic cooperativity). Each conformational state has up to n binding sites for ligand *A*. The conformational landscape of the protein will be altered by the presence of ligand *A*: Depending on the ligand binding capabilities (overall association constants and stoichiometry) of the different conformational states P_s, their population will increase, if ligand *A* binds preferentially, or decrease, if ligand *A* does not bind preferentially or does not bind at all. Projecting downward or rightward, and performing the appropriate renormalization of the binding polynomial, this complex scenario is converted into a quasi-simple conformational equilibrium or a protein–ligand binding equilibrium (Eqs. 7–8), thus reducing the apparent complexity of the system. However, the complexity of the system remains in the apparent equilibrium constants (Eqs. 7–8)

$$q_k = V_0[P]_{\mathrm{T,k}}\left(\langle\Delta H\rangle_{\mathrm{k}} - \langle\Delta H\rangle_{\mathrm{k-1}}\right) = V_0\sum_{s=0}^{t}\sum_{i=0}^{n}\Delta H_{\mathrm{si}}\left([P_sA_i]_{\mathrm{k}} - [P_sA_i]_{\mathrm{k-1}}\left(1-\frac{v}{V_0}\right)\right) \quad (6)$$

where V_0 is the calorimetric cell volume and v is the injection volume. Nonlinear least squares regression data analysis of the binding isotherm allows estimating the overall binding parameters (β_{si}'s and ΔH_{is}'s).

Not all overall association constants are independent; because of the energy conservation principle, for each square we can define in the global chart one of the constants depends on the other three ones. In addition, and fortunately, not all conformational states are able to bind the ligand *A*, and therefore, most of the β_{si}'s are equal to zero. There might be significant differences in binding affinity among the conformational states able to bind ligand *A*, and therefore, additional simplifications can be made if certain low-affinity binding states can be neglected. This kind of simplifications was previously assumed in the Monod–Wyman–Changeux (MWC) model [10] and the Koshland–Nemethy–Filmer (KNF) model [22], where the general allosteric model is strongly simplified to a reduced number of statistically and biologically significant protein states.

A different kind of simplification can be applied if the binding polynomial is renormalized as follows, by projecting downward the general chart (Fig. 2):

$$Z = \frac{\sum_{s=0}^{t}\sum_{i=0}^{n}\beta_{\mathrm{si}}\gamma_s[A]^{\mathrm{i}}}{\sum_{\mathrm{i}}^{n}\beta_{0\mathrm{i}}[A]^{\mathrm{i}}} = \sum_{s=0}^{t}\gamma_s\frac{\sum_{i=0}^{n}\beta_{\mathrm{si}}[A]^{\mathrm{i}}}{\sum_{i=0}^{n}\beta_{0\mathrm{i}}[A]^{\mathrm{i}}} = \sum_{s=0}^{t}\gamma_s\frac{Z_{\mathrm{s,A}}}{Z_{\mathrm{0,A}}} = \sum_{s=0}^{t}\gamma_s^{\mathrm{app}} \quad (7)$$

Any renormalization is performed by dividing the binding polynomial by a set of terms representing a specific subset of protein states, a subensemble that will be considered as a reference for the thermodynamic potentials and whose thermodynamic parameters will be implicitly considered within apparent parameters. Therefore, in practice any renormalization will consist of a simplification of the protein conformational and functional landscape by focusing only on a specific aspect of that system, while keeping implicitly other secondary aspects. In fact, the renormalization leading to a simplification in the binding polynomial is commonly and implicitly assumed when the description of the system is just based on one specific aspect, either conformational equilibrium or ligand binding equilibrium. In Eq. 7, the subensemble of P_0A_i states (that is, the native state with any number of ligand *A* molecules bound) has been taken as a reference, and *Z* is simplified by focusing the description just on the protein conformational

equilibrium and keeping ligand binding "hidden" into apparent conformational constants γ_s^{app}. $Z_{s,A}$ is the subpolynomial restricted to the subensemble of P_s conformation with any number of ligand A molecules bound, and γ_s^{app} is the apparent conformational equilibrium constant for the P_s conformation. This expression for Z is used when studying the conformational equilibrium of a protein and assessing the influence of ligand A binding. The effect of ligand A binding is contained within the apparent conformational constants. Equation 7 indicates that the apparent conformational equilibrium constant for the P_s conformation, γ_s^{app}, is equal to that constant in the absence of ligand A modulated by two factors: the ligand A-dependent binding subpolynomials for P_s and P_0 conformations.

Another simplification can be applied if the binding polynomial is renormalized as follows, by projecting the general chart rightward (Fig. 2):

$$Z = \frac{\sum_{s=0}^{t}\sum_{i=0}^{n}\beta_{si}\gamma_s[A]^i}{\sum_{s=0}^{t}\gamma_s} = \sum_{i=0}^{n}\frac{\sum_{s=0}^{t}\beta_{si}\gamma_s}{\sum_{s=0}^{t}\gamma_s}[A]^i = \sum_{i=0}^{n}\beta_i^{app}[A]^i \quad (8)$$

In this expression, the subensemble of ligand A-free P_s conformation states (that is, any conformational state with no ligand A molecules bound) has been taken as a reference, and Z is simplified by focusing the description just on the ligand binding equilibrium and keeping the conformational equilibrium "hidden" into apparent binding constants β_i^{app}. Thus, β_i^{app} is the apparent overall association constant for the complex with i molecules of ligand A bound. This expression for Z is used when studying the ligand binding equilibrium of a protein and assessing the influence of conformational equilibrium. The effect of the conformational equilibrium is contained within the apparent binding constants. Equation 8 indicates that the apparent overall binding constant for the PA_i complex, β_i^{app}, is the population-weighted average of the individual binding constants within the subensemble of P_sA_i complexes.

The general allosteric model: two ligand binding equilibria

The binding polynomial can also be generalized for a macromolecule able to bind two ligands, A with n sites and B with m sites (Fig. 3) [1]:

$$Z = \sum_{i=0}^{n}\sum_{j=0}^{m}\frac{[PA_iB_j]}{[P]} = \sum_{i=0}^{n}\sum_{j=0}^{m}\beta_{ij}[A]^i[B]^j \quad (9)$$

where β_{ij} is the overall association constant for the complex PA_iB_j. The constant β_{ij} can be conveniently split into two factors: $\beta_{ij} = \beta_{i0}\beta_{j/i}$, where β_{i0} is the overall association constant for $P + A_i \leftrightarrow PA_i$ and $\beta_{j/i}$ is the overall association constant for $PA_i + B_j \leftrightarrow PA_iB_j$. Furthermore, the constant $\beta_{j/i}$ can be factorized as: $\beta_{j/i} = \beta_{0j}\alpha_{ij}$, where α_{ij} accounts for the reciprocal (see "Appendix") heterotropic cooperative effect between ligand A and ligand B binding (with $\alpha_{i0} = \alpha_{0j} = 1$; that is, there is no heterotropy between molecules of the same ligand). Depending on the value of α_{ij}, the binding of ligand A and ligand B will be independent ($\alpha_{ij} = 1$) or cooperative ($\alpha_{ij} \neq 1$). The homotropy between identical ligands is accounted for within β_{i0} and β_{0j} (Eq. 4). The fraction or population of each protein species in equilibrium is expressed as:

$$\chi_{ij} = \frac{[PA_iB_j]}{Z} = \frac{\beta_{ij}[A]^i[B]^j}{Z} = \frac{\beta_{i0}\beta_{0j}\alpha_{ij}[A]^i[B]^j}{Z} \quad (10)$$

and the main averages can be calculated directly or through the first derivatives of the partition function:

$$\begin{aligned}\langle\Delta G\rangle &= -RT\ln Z\\ n_{LB,A} &= \sum_{i=0}^{n}\sum_{j=0}^{m} i\chi_{ij} = \left(\frac{\partial \ln Z}{\partial \ln[A]}\right)_{T,p,[B]\ldots}\\ n_{LB,B} &= \sum_{i=0}^{n}\sum_{j=0}^{m} j\chi_{ij} = \left(\frac{\partial \ln Z}{\partial \ln[B]}\right)_{T,p,[A]\ldots}\\ \langle\Delta H\rangle &= \sum_{i=0}^{n}\sum_{j=0}^{m}\Delta H_{ij}\chi_{ij} = RT^2\left(\frac{\partial \ln Z}{\partial T}\right)_{p,[A],[B]\ldots}\end{aligned} \quad (11)$$

where $\langle\Delta G\rangle$ is the excess average Gibbs energy of the system containing specifically the contribution of ligand A and ligand B binding, $n_{LB,A}$ and $n_{LB,B}$ are the average numbers of ligand A and ligand B molecules bound per protein molecule, ΔH_{ij} is the overall binding enthalpy associated with the formation of complex PA_iB_j and $\langle\Delta H\rangle$ is the excess average binding enthalpy of the system. It is important to realize that Eq. 11 represent generalizations of the usual link between the equilibrium constant and ΔG, and the van't Hoff equation or the Gibbs–Helmholtz equation.

Again, the overall stoichiometric association constants β_{i0}'s and β_{0j}'s can be expressed as a function of the total number of binding sites, n or m, the number of ligand A and ligand B molecules bound per macromolecule, i or j, the first stoichiometric association constants for ligand A and ligand B, β_{01} or β_{10} (or the intrinsic site-specific association constants, K_A and K_B), and the cooperativity constant accounting for homotropic cooperativity effects for ligand A or ligand B binding, α_i^A or α_i^B:

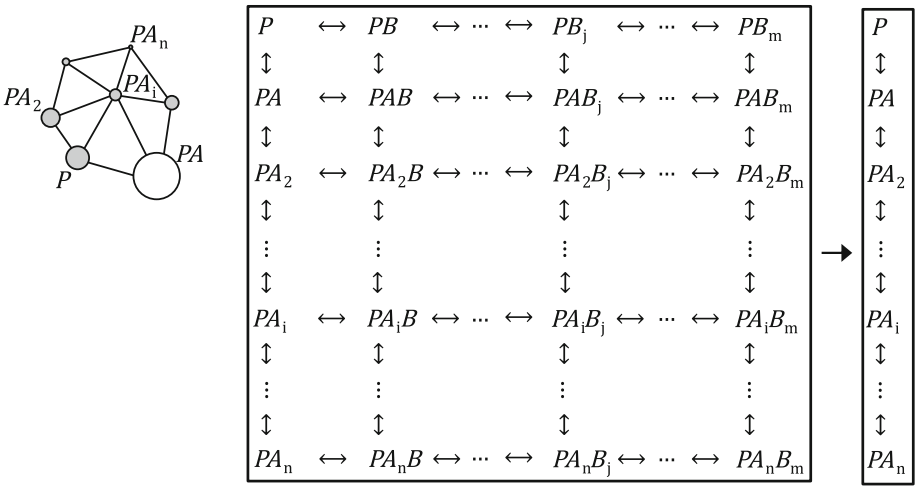

Fig. 3 Chart corresponding to the general allosteric model for the coupling of the binding of two different ligand bindings (heterotropic cooperativity). Each conformational state has up to n binding sites for ligand *A* and up to m binding sites for ligand *B*. The landscape of the protein will be altered by the presence of ligand *B*: Depending on the ligand *B* binding capabilities (overall association constants and stoichiometry) of the different complexes PA_i, their population will be increase, if ligand *B* binds preferentially, or decrease, if ligand *B* does not bind preferentially or does not bind at all. Projecting rightward, and performing the appropriate renormalization of the binding polynomial, this complex scenario is converted into a quasi-simple protein–ligand binding equilibrium (Eq. 15), thus reducing the apparent complexity of the system. However, the complexity of the system remains in the apparent equilibrium constants for ligand *A* (Eq. 15)

$$\begin{aligned}\beta_{i0} &= \binom{n}{i} n^{-i} \beta_{10}^{i} \alpha_{i}^{A} \\ \beta_{0j} &= \binom{m}{j} m^{-j} \beta_{01}^{j} \alpha_{j}^{B}\end{aligned} \tag{12}$$

The binding equations are obtained when considering the chemical equilibrium (basically, the binding polynomial) together with the mass conservation principle:

$$\begin{aligned}[A]_T &= [A] + [P]_T n_{LB,A} = [A] + [P]_T \frac{\partial \ln Z}{\partial \ln [A]} \\ [B]_T &= [B] + [P]_T n_{LB,B} = [B] + [P]_T \frac{\partial \ln Z}{\partial \ln [B]} \\ [P]_T &= [P] Z\end{aligned} \tag{13}$$

and the calorimetric equation provides the heat effect, q, per individual injection k (binding isotherm) when injecting ligand *A* into protein P in the presence of ligand *B*:

$$\begin{aligned}q_k &= V_0 [P]_{T,k} \left(\langle \Delta H_k \rangle - \langle \Delta H \rangle_{k-1} \right) \\ &= V_0 \sum_{i=0}^{n} \sum_{j=0}^{m} \Delta H_{ij} \left(\left[PA_i B_j \right]_k - \left[PA_i B_j \right]_{k-1} \left(1 - \frac{v}{V_0} \right) \right)\end{aligned} \tag{14}$$

where V_0 is the calorimetric cell volume and v is the injection volume. Nonlinear least squares regression data analysis of the binding isotherm allows estimating the overall binding parameters (β_{ij}'s and ΔH_{ij}'s).

Not all overall association constants are independent; because of the energy conservation principle, for each square we can define in the global chart one of the constants depends on the other three ones. In addition, and fortunately, not all ligand *A* complexes would be able to bind the ligand *B*, and therefore, many β_{ij} are equal to zero (especially in the case of competitive ligands). There might be significant differences in binding affinity for ligand *B* among the ligand *A* complexes states, and therefore, additional simplifications can be made if certain low-affinity binding states can be neglected.

The binding polynomial can be renormalized as follows, by projecting the general chart rightward (Fig. 3):

$$\begin{aligned}Z &= \frac{\sum_{i=0}^{n} \beta_{i0} [A]^i \sum_{j=0}^{m} \beta_{0j} \alpha_{ij} [B]^j}{\sum_{j=0}^{m} \beta_{0j} [B]^j} = \sum_{i=0}^{n} \beta_{i0} \frac{Z_{i,B}}{Z_{0,B}} [A]^i \\ &= \sum_{i=0}^{n} \beta_i^{app} [A]^i\end{aligned} \tag{15}$$

In this expression, the subensemble of ligand *A*-free states PB_j (that is, any complex with any ligand *B* molecules and no ligand *A* bound) has been taken as a reference, and *Z* is simplified by focusing the description just on ligand *A* binding equilibrium, keeping the other ligand *B* binding equilibrium "hidden" into apparent binding constants β_i^{app}. $Z_{i,B}$ is the binding subpolynomial restricted to the subensemble of state PA_iB_j with any ligand *B* molecules bound and just i ligand *A* molecules bound, and β_i^{app} is the apparent association constant for the subensemble of states with *i* ligand *A* molecules bound. Equation 15 indicates that the apparent overall binding constant for the state PA_i, β_i^{app}, is equal to that constant in the absence of ligand

B modulated by two factors: the ligand B-dependent binding subpolynomials for states PA_i and P.

The simplifications of the coupling between different equilibria contained in Eqs. 7, 8 and 15 indicate that apparent conformational and binding equilibrium constants can be employed and the complexity of the system is reduced considerably. This is usually done when studying the conformational stability or the interaction of a given protein as a function of certain ligand (e.g., protons, salt ions, cofactor, small molecule, another protein). Using apparent binding parameters allows reducing a complex system and its binding equations (Eq. 13) to a simpler system (Eq. 5). Using just apparent equilibrium constants will provide very useful, but partial and incomplete, information, as it will be shown below, and in order to get additional insight into the energetics of the cooperative and allosteric affects, the explicit functional dependence of the apparent equilibrium constants on the concentration of the additional ligand must be taken into account. The apparent binding parameters contain implicitly the influence of the additional ligand, and when convenient and possible, they allow estimating the cooperativity parameters.

Of course, the binding polynomial can be further generalized in a straightforward manner for a protein exhibiting a conformational equilibrium and able to bind two different ligands. Similar simplifications are constructed by projecting appropriately the three-dimensional (conformation, ligand A and ligand B) general chart for the general allosteric model. As it will be shown in the next section, each simplification of the general allosteric model leads to a linkage relationship.

Linkage relationships

It can be concluded from Eq. 7 that:

$$\gamma_s^{app} = \gamma_s \frac{Z_{s,A}}{Z_{0,A}}$$
$$\Delta G_s^{app} = \Delta G_s + \langle \Delta G_{s,A} \rangle - \langle \Delta G_{0,A} \rangle$$
$$\left(\frac{\partial \ln \gamma_s^{app}}{\partial \ln [A]} \right)_{T,p,\ldots} = n_{LB,s,A} - n_{LB,0,A} = \Delta n_{LB,s,A}$$
$$RT^2 \left(\frac{\partial \ln \gamma_s^{app}}{\partial T} \right)_{[A],p,\ldots} = \Delta H_s^{app} = \Delta H_s + \langle H_{s,A} \rangle - \langle H_{0,A} \rangle \quad (16)$$

where $n_{LB,s,A}$ is the average number of ligand A molecules bound per protein molecule in the subensemble of the P_s conformation, ΔG_s and ΔH_s are the conformational Gibbs energy and enthalpy for the P_s conformation, and $\langle \Delta G_{s,A} \rangle$ and $\langle \Delta H_{s,A} \rangle$ are the excess average ligand binding Gibbs energy and the enthalpy for ligand A in the subensemble of the P_s conformation. Equations 16 contain well-known linkage relationships between conformational equilibrium and ligand binding [1].

The population of the conformational state P_s in the absence of ligand A is given by:

$$\chi_s = \frac{\gamma_s}{\sum_{s=0}^{t} \gamma_s} \quad (17)$$

but in the presence of a certain concentration of ligand A is given by:

$$\chi_s = \sum_{i=0}^{n} \chi_{si} = \frac{\sum_{i=0}^{n} \beta_{si} \gamma_s [A]^i}{\sum_{s=0}^{t} \sum_{i=0}^{n} \beta_{si} \gamma_s [A]^i} = \gamma_s \frac{Z_{s,A}}{Z} \quad (18)$$

and the total Gibbs energy associated with that conformation P_s (intrinsic conformational energy plus that provided by ligand A binding) considering the conformation P_0 as a reference, is given by (see Eq. 16):

$$\Delta G_s^{app} = -RT \ln \gamma_s - RT \ln \left(\sum_{i=0}^{n} \beta_{si} [A]^i \right) + RT \ln \left(\sum_{i=0}^{n} \beta_{0i} [A]^i \right) \quad (19)$$

Interestingly, from Eq. 16, the conformational equilibrium constant will depend on ligand A if there is a difference in the binding extent for ligand A between conformation P_s and P_0 (i.e., if $\beta_{si} > \beta_{0i}$ or $\beta_{si} < \beta_{0i}$):

$$\left(\frac{\partial \ln \gamma_s^{app}}{\partial \ln [A]} \right)_{T,p,\ldots} = \Delta n_{LB,s,A} = \frac{\sum_{i=0}^{n} i \beta_{si} [A]^i}{\sum_{i=0}^{n} \beta_{si} [A]^i} - \frac{\sum_{i=0}^{n} i \beta_{0i} [A]^i}{\sum_{i=0}^{n} \beta_{0i} [A]^i} \quad (20)$$

These last equations (Eqs. 19 and 20) indicate that ligand A binding will elicit a decrease or an increase in the overall Gibbs energy for conformation P_s, or ligand A will promote the forward or backward $P_0 \leftrightarrow P_s$ process, depending on the relative affinity for conformation P_s compared to that of conformation P_0: If ligand A binds preferentially to conformation P_s ($\beta_{si} > \beta_{0i}$), the overall Gibbs energy of conformation P_s is reduced and its population is increased, promoting the conformational transition from P_0 to P_s; if ligand A binds preferentially to conformation P_0 ($\beta_{si} < \beta_{0i}$), the overall Gibbs energy of conformation P_s is increased and its population is decreased, promoting the conformational transition from P_s to P_0.

It can be concluded from Eq. 14 that:

$$\beta_{\mathrm{i}}^{\mathrm{app}} = \beta_{\mathrm{i0}} \frac{Z_{\mathrm{i,B}}}{Z_{\mathrm{0,B}}}$$
$$\Delta G_{\mathrm{i}}^{\mathrm{app}} = \Delta G_{\mathrm{i0}} + \langle \Delta G_{\mathrm{i,B}} \rangle - \langle \Delta G_{\mathrm{0,B}} \rangle$$
$$\left(\frac{\partial \ln \beta_{\mathrm{i}}^{\mathrm{app}}}{\partial \ln [B]} \right)_{\mathrm{T,p,...}} = n_{\mathrm{LB,i,B}} - n_{\mathrm{LB,0,B}} = \Delta n_{\mathrm{LB,i,B}}$$
$$RT^2 \left(\frac{\partial \ln \beta_{\mathrm{i}}^{\mathrm{app}}}{\partial T} \right)_{\mathrm{[B],p,...}} = \Delta H_{\mathrm{i}}^{\mathrm{app}} = \Delta H_{\mathrm{i0}} + \langle \Delta H_{\mathrm{i,B}} \rangle - \langle \Delta H_{\mathrm{0,B}} \rangle \tag{21}$$

where $n_{\mathrm{LB,i,B}}$ is the average number of ligand B molecules bound per protein molecule in the subensemble of states with i molecules of ligand A bound, ΔG_{i0} and ΔH_{i0} are the binding Gibbs energy and enthalpy for the complex PA_{i}, and $\langle \Delta G_{\mathrm{i,B}} \rangle$ and $\langle \Delta H_{\mathrm{i,B}} \rangle$ are the excess average binding Gibbs energy and the enthalpy for ligand B in the subensemble of states with i molecules of ligand A bound. Equation 21 contains well-known linkage relationships for the coupling of the binding of two ligands [1].

The population of a given ligation state PA_{i} in the absence of ligand B is given by:

$$\chi_{\mathrm{i}} = \frac{\beta_{\mathrm{i}} [A]^{\mathrm{i}}}{\sum_{\mathrm{i}=0}^{n} \beta_{\mathrm{i}} [A]^{\mathrm{i}}} \tag{22}$$

but in the presence of a certain concentration of ligand B is given by:

$$\chi_{\mathrm{i}} = \sum_{\mathrm{j}=0}^{m} \chi_{\mathrm{ij}} = \frac{\sum_{\mathrm{j}=0}^{m} \beta_{\mathrm{i0}} \beta_{\mathrm{0j}} \alpha_{\mathrm{ij}} [A]^{i} [B]^{j}}{\sum_{\mathrm{i}=0}^{n} \sum_{\mathrm{j}=0}^{m} \beta_{\mathrm{ij}} [A]^{i} [B]^{j}} = \beta_{\mathrm{i0}} [A]^{i} \frac{Z_{\mathrm{i,B}}}{Z} \tag{23}$$

and the total Gibbs energy associated with complex PA_{i} (intrinsic energy plus that provided by ligand B binding), considering the ligand A-free subensemble as a reference, is given by (see Eq. 21):

$$\Delta G_{\mathrm{i}}^{\mathrm{app}} = -RT \ln \beta_{\mathrm{i0}} - RT \ln \left(\sum_{\mathrm{j}=0}^{m} \beta_{\mathrm{0j}} \alpha_{\mathrm{ij}} [B]^{j} \right) + RT \ln \left(\sum_{\mathrm{j}=0}^{m} \beta_{\mathrm{0j}} [B]^{j} \right) \tag{24}$$

Interestingly, from Eq. 21, the conformational equilibrium constant will depend on ligand B if there is a difference in the binding extent for ligand B between complex PA_{i} and ligand A-free P (i.e., if $\alpha_{\mathrm{ij}} > 1$ or $\alpha_{\mathrm{ij}} < 1$):

$$\left(\frac{\partial \ln \beta_{\mathrm{i}}^{\mathrm{app}}}{\partial \ln [B]} \right)_{\mathrm{T,p,[A]...}} = \Delta n_{\mathrm{LB,i,B}} = \frac{\sum_{i=0}^{m} j \beta_{\mathrm{0j}} \alpha_{\mathrm{ij}} [B]^{j}}{\sum_{j=0}^{m} \beta_{\mathrm{0j}} \alpha_{\mathrm{ij}} [B]^{j}} - \frac{\sum_{i=0}^{m} j \beta_{\mathrm{0j}} [B]^{j}}{\sum_{j=0}^{m} \beta_{\mathrm{0j}} [B]^{j}} \tag{25}$$

These last equations (Eqs. 24 and 25) indicate that ligand B binding will elicit a decrease or an increase in the overall Gibbs energy for complex PA_{i}, or ligand B will promote the forward or backward $P \leftrightarrow PA_{\mathrm{i}}$ process, depending on the relative affinity of state PA_{i} for ligand B compared to that of ligand A-free P: If ligand B binds preferentially to complex PA_{i} ($\alpha_{\mathrm{ij}} > 1$), the overall Gibbs energy of complex PA_{i} is decreased and its population is increased, promoting the ligand A association from P to PA_{i}; if ligand binds preferentially to ligand A-free P ($\alpha_{\mathrm{ij}} < 1$), the overall Gibbs energy of complex PA_{i} is increased and its population is decreased, promoting ligand A dissociation from PA_{i} to P.

General linkage relationship

Considering ligand A as the primary ligand and ligand B as the secondary ligand, it is obvious that Eqs. 16 and 21 share a common starting point:

$$K_{\mathrm{eq}}^{\mathrm{app}}([B]) = K_{\mathrm{eq}} \frac{Z_{\mathrm{q,B}}}{Z_{\mathrm{0,B}}} \tag{26}$$

where $K_{\mathrm{eq}}^{\mathrm{app}}([B])$ is an apparent equilibrium constant (either a conformational constant $\gamma_{\mathrm{s}}^{\mathrm{app}}$ for the process $P_0 \leftrightarrow P_{\mathrm{s}}$, or a binding constant $\beta_{\mathrm{i}}^{\mathrm{app}}$ for the process $P + iA \leftrightarrow PA_{\mathrm{i}}$) in the presence of secondary ligand B and, therefore, dependent on ligand B concentration and affinity. K_{eq} is the intrinsic equilibrium constant in the absence of secondary ligand B, and the multiplying factor is the quotient of two binding subpolynomials, accounting for the details of the coupling between conformational and ligand B binding equilibria or between ligand A and ligand B binding equilibria. Deriving with respect to ligand B concentration, the following expression can be obtained:

$$\left(\frac{\partial \ln K_{\mathrm{eq}}^{\mathrm{app}}([B])}{\partial \ln [B]} \right)_{\mathrm{T,p,...}} = \Delta n_{\mathrm{LB,B}} \tag{27}$$

which indicates that the equilibrium constant for a given process between two states and associated with conformational transition or complex formation will depend on ligand B concentration if the binding extent for ligand B (number of ligand B molecules bound per protein molecule) is different between the final and initial states of the process.

This general linkage equation can be employed for establishing conservation and variation theorems for $K_{\mathrm{eq}}^{\mathrm{app}}$:

- $K_{\mathrm{eq}}^{\mathrm{app}}$ is constant (does not depend on ligand B concentration) if and only if $\Delta n_{\mathrm{LB,B}}$ is zero. This will occur if ligand B does not bind to any of the two states, or if

ligand B binds equally to both states (i.e., $\beta_{si} = \beta_{0i}$, or $\alpha_{ij} = 1$) with no allosteric and cooperative effect.

- K_{eq}^{app} is not constant (depends on ligand B concentration) if and only if $\Delta n_{LB,B}$ is nonzero. This will occur if ligand B binds preferentially to any of the two states (i.e., $\beta_{si} \neq \beta_{0i}$ or $\alpha_{ij} \neq 1$) through an allosteric and cooperative fashion.

These statements derived from Eq. 27 represent the mathematical formulation of the already stated principle for which a ligand will stabilize and increase the population of those (conformational or ligand A bound) states the ligand binds preferentially to.

The relevance and power of Eq. 27 lie in its simplicity. No matter what the intricacies of the conformational equilibrium or the interaction with ligand A are, and what underlying complexities of the coupling with ligand B there are, this relationship provides information on the influence of ligand B on a certain conformational change or a certain binding process. The quantity $\Delta n_{LB,B}$ is the net difference in the binding extent of ligand B between two protein states. $\Delta n_{LB,B}$ can be a fractional number, because it is the difference between two fractional numbers. The binding extent, n_{LB}, is a statistical average number of ligand molecules bound per protein molecule. For that reason, $\Delta n_{LB,B}$ does not provide direct quantitative information on the cooperativity or allosteric effect; it is not possible to infer the differences in ligand B affinities between conformational states, i.e., β_{si} and β_{0i}, or between complexes, i.e., α_{ij}. However, it provides semiquantitative and very useful information: $\Delta n_{LB,B}$ indicates whether β_{si} is larger or smaller than β_{0i}, or whether α_{ij} is larger or smaller than 1. In addition, it allows estimating how much K_{eq}^{app} will vary for a relatively small variation in ligand B concentration, by integrating Eq. 27, and considering $\Delta n_{LB,B}$ constant within a small ligand B concentration range:

$$K_{eq}^{app}([B]) = K_{eq}^{app}([B]_0)\left(\frac{[B]}{[B]_0}\right)^{\Delta n_{LB,B}}$$
$$\frac{\Delta K_{eq}^{app}([B])}{K_{eq}^{app}([B])} = \Delta n_{LB,B}\frac{\Delta[B]}{[B]} \quad (28)$$

The reason for stating "a relatively small variation in ligand B" is that, if different binding sites for ligand B, with different binding affinities and different contributions to $\Delta n_{LB,B}$, are present, then a non-constant $\Delta n_{LB,B}$ value along the practical range of ligand B concentration arises. The parameter $\Delta n_{LB,B}$ is related to the number of ligand B binding sites (m), but it does not report such number. Only in the case of almost no binding to one of the states and high affinity to the other state linked by K_{eq} ($\beta_{si} \approx 0$ and large β_{0i}, or $\beta_{0i} \approx 0$ and large β_{j0}), or in the case of high cooperativity ($\alpha_{ij} \gg 1$ or $\alpha_{ij} \ll 1$), $\Delta n_{LB,B}$ will be close to m at some ligand B concentration. The absolute value of $\Delta n_{LB,B}$ is a lower bound for m ($m \geq |\Delta n_{LB,B}|$).

In the case of an allosteric effect, the influence of ligand B on γ_s^{app} will be maximal at an intermediate ligand B concentration in the order of the overall dissociation constants (see "Appendix"). For very low or very high ligand B concentrations, $\Delta n_{LB,s,B}$ will be close to zero because the ligand B binding extent to both states, P_s and P_0, will be similarly small or large. Likewise, in the case of a heterotropic effect, the influence of ligand B on β_{i0}^{app} will be maximal at an intermediate ligand B concentration in the order of the overall dissociation constants (see "Appendix"). For very low or very high ligand B concentrations, $\Delta n_{LB,B}$ will be close to 0 because the ligand B binding extent to both states, PA_i and P, will be similarly small or large. In both cases, allostery and heterotropy, the maximal value of $\Delta n_{LB,z,X}$ ($z \equiv s$ or i, $X \equiv A$ or B) occurs at the concentration of ligand X for which the derivative of $\Delta n_{LB,z,X}$ with respect to ligand X concentration vanishes (i.e., the binding capacity of the protein for ligand X [1, 23] is the same for both linked states, either P_s and P_0, or PA_i and P).

The quantity $\Delta n_{LB,B}$ is experimentally accessible by constructing the Wyman plot: measuring K_{eq}^{app} (conformational stability constant or binding affinity constant for ligand A) as a function of ligand B concentration and plotting $\ln(K_{eq}^{app})$ versus $\ln([B])$. Thus, the slope of the plot is $\Delta n_{LB,B}$.

The connection of Eqs. 27 and 28 with the Le Chatelier's principle is obvious: If a process characterized by an equilibrium constant K_{eq}^{app} is coupled to the association/dissociation of ligand B through a net quantity $\Delta n_{LB,B}$, a change in the concentration of ligand B will trigger a shift in the overall equilibrium favoring certain protein (conformational and ligand A bound) states according to the magnitude and sign of $\Delta n_{LB,B}$.

Other interesting linkage relationships can be obtained from the application of Legendre transformations and Maxwell relationships to the binding potential [1, 4].

Example 1: Glt_{Ph} shows heterotropic aspartate and sodium ions binding cooperativity

Glt_{Ph} is an archeal homologue of mammalian glutamate transporters that co-transports by symport an aspartate molecule together with sodium ions [24, 25]. The favorable internalization of sodium through its electrochemical gradient provides energy for internalization of aspartate into the cytoplasm against its concentration gradient. Aspartate and sodium hardly bind to Glt_{Ph} in the absence of each other ligand. However, both ligands bind to the transporter with high positive cooperativity [26], where a remarkable

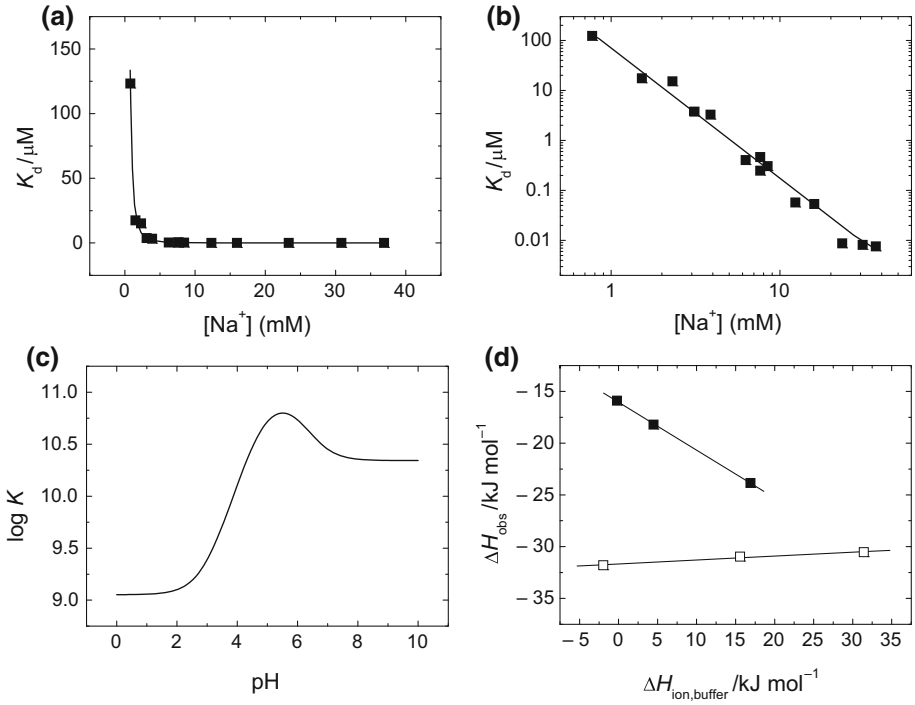

Fig. 4 **a** Dependency of the dissociation constant K_d for aspartate binding to trimeric Glt_{Ph} as a function of sodium ion concentration. The dissociation constant for aspartate, determined by isothermal titration calorimetry and fluorescence spectroscopy, shows a marked dependency on sodium concentration, indicating a heterotropic cooperativity effect between aspartate and sodium [26]. **b** The Wyman plot allows estimating the net difference in the binding extent of sodium between the aspartate-bound Glt_{Ph} and aspartate-free Glt_{Ph} ($\partial \ln K_{d,asp}/\partial \ln[Na^+] = -\Delta n_{LB,Na}$): $\Delta n_{LB,Na} = 2.6$, which indicates that the binding of at least 3 sodium ions occurs cooperatively with the binding of an aspartate molecule to each of the three subunits in Glt_{Ph} [26]. **c** Dependency of the association constant, K, for the interaction of the inhibitor KNI-272 with the HIV-1 protease. The association constant is not constant along the pH range, indicating that the binding of the inhibitor is coupled to the de/protonation of certain functional groups (heterotropic cooperativity between inhibitor and protons) [29]. The slope of the Wyman plot at any pH is equal to the net difference in proton binding extent, $\Delta n_{LB,H}$ between the inhibitor-bound state and the inhibitor-free state ($\partial \log K/\partial pH = -\Delta n_{LB,H}$) at that pH. From pH 0 to pH 5.5 a deprotonation event ($\Delta n_{LB,H} < 0$) dominates the pH dependency of the inhibitor association constant, while from pH 5.5 to pH 10 a protonation event ($\Delta n_{LB,H} > 0$) dominates that dependency. **d** Experiments performed at the same pH with buffers with different ionization enthalpies allowed estimating $\Delta n_{LB,H}$ and ΔH_0 for KNI-272 binding to HIV-1 protease from linear regression data analysis (Eq. 29). Experimental data (observed experimental enthalpy of interaction) at pH 3.6 revealing $\Delta n_{LB,H} < 0$ (closed squares) and at pH 6 revealing $\Delta n_{LB,H} > 0$ (open squares) as a function of the buffer ionization enthalpy are shown

increase in affinity (aspartate dissociation constant K_d from 120 μM to 8 nM) is observed in a very small sodium concentration range (Fig. 4a). The three aspartate binding sites in this trimeric protein seem to behave as identical and independent, and therefore, $K_d = 1/K = 3/\beta_1$ (see Eq. 47). The constant slope observed in the Wyman plot ($\partial \ln K_{d,asp}/\partial \ln[Na^+] = -\Delta n_{LB,Na}$) indicates that the three binding sites for sodium in each subunit display identical binding association constants (or they bind with very high homotropic cooperativity) and that, within the experimental range employed for sodium, the binding of aspartate results in the same net change in the binding extent of sodium between the aspartate-bound transporter and the aspartate-free transporter, $\Delta n_{LB,Na}$ (Fig. 4b). For much higher sodium concentrations (much more than its intrinsic dissociation constant, which is larger than 100 mM), $\Delta n_{LB,Na}$ would be diminished because of a larger preexisting sodium saturation fraction for the aspartate-free transporter. It can be concluded that: (1) aspartate and sodium show positive heterotropic cooperativity ($\Delta n_{LB,Na} \neq 0$); (2) sodium binds preferentially to the aspartate-bound transporter ($\Delta n_{LB,Na} > 0$); (3) at least three sodium ions bind to each transporter subunit ($m \geq 2.6$); and (4) a ten-fold difference in sodium concentration leads to a 400-fold difference in aspartate affinity (according to Eq. 28).

Example 2: pH dependence of inhibitor binding to HIV-1 protease

HIV-1 protease is one of the main targets for therapeutic intervention against AIDS [27, 28]. KNI-272 belongs to the family of allophenylnorstatine derivatives exhibiting enthalpically driven binding to this enzyme [29]. Because this enzyme has a single binding site for the ligand,

$\beta_1 = K$ (see Eq. 47). According to an exhaustive characterization of the inhibitor interaction as a function of pH, it was found that the binding of the inhibitor is linked to the protonation/deprotonation of two ionizable groups [29]. In the free reactants state, these groups have pK_a's of 6.0 and 4.8, shifting to 6.6 and 2.9 in the bound reactant state. These groups were identified as one of the aspartates in the catalytic dyad in the protease (becoming protonated upon inhibitor binding) and the isoquinoline nitrogen in the inhibitor molecule (becoming deprotonated upon inhibitor binding). The changes in pK_a's (changes in proton affinity) experienced by those groups as a result of inhibitor binding and the change in inhibitor affinity as a result of proton association/dissociation reflect the reciprocal heterotropic cooperative effect between proton and inhibitor binding. The variable slope observed in the Wyman plot (Fig. 4c) indicates that $\Delta n_{LB,H}$ is not a constant quantity because there are two groups involved in the proton exchange process, with different proton affinities (different pK_a's) and with different cooperative effects and susceptibilities (undergoing different pK_a changes), resulting in a different binding extent of protons (proton saturation fraction) to the inhibitor-free and inhibitor-bound states at different pHs.

It can be concluded that: (1) inhibitor and protons show negative heterotropic cooperativity at acidic pH (deprotonation upon binding, $\Delta n_{LB,H} < 0$) and positive heterotropic cooperativity at neutral pH (protonation upon binding, $\Delta n_{LB,H} > 0$); (2) at acidic pH protons bind preferentially to the inhibitor-free state ($\Delta n_{LB,H} < 0$), while at neutral pH protons bind preferentially to the inhibitor-bound state ($\Delta n_{LB,H} > 0$); (3) at least two ionizable groups are involved in the proton exchange process (not because of the magnitude of $\Delta n_{LB,H}$, but because of the biphasic shape observed in Fig. 4c); (4) along the deprotonation at acidic pH, a pH change of 1 unit or a tenfold difference in free proton concentration leads to a sixfold difference in inhibitor affinity, while along the protonation at neutral pH, a pH change of 1 unit leads to a twofold difference in inhibitor affinity (according to Eq. 28) and (5) the maximal inhibitor binding affinity is observed around pH 5–6 ($\Delta n_{LB,H} \approx 0$).

The quantity $\Delta n_{LB,H}$ can be more conveniently determined by performing calorimetric titrations using buffers with similar pK_a and different ionization enthalpies (Fig. 4d). The observed interaction enthalpy, ΔH_{obs}, can be plotted as a function of the ionization enthalpy of the buffer employed, $\Delta H_{ion,buffer}$, and $\Delta n_{LB,H}$ and ΔH_0 (buffer-independent ligand binding enthalpy) can be readily estimated as the slope and y-axis intercept from linear regression analysis:

$$\Delta H_{obs} = \Delta H_0 + \Delta n_{LB,H} \Delta H_{ion,buffer} \tag{29}$$

A detailed analysis of $\Delta n_{LB,H}$ and ΔH_0 as a function of pH allowed dissecting the proton exchange contributions to the overall inhibitor binding energetics and outlining the pH dependency of the inhibitor association constant (Fig. 4c) [29]. Proton exchange coupling is a specific, widespread example of heterotropic cooperativity in proteins. If a protein has a single ligand binding site for a ligand (with association constant $K = \beta_1$), and m protonation sites (in the protein or in the ligand) that undergo changes in their pK_a from $pK_{a,j}^{free}$ to $pK_{a,j}^{bound}$ upon ligand binding, Eqs. 21–25 can be translated to a more familiar form:

$$\begin{aligned}
K^{app} &= K \frac{\prod_{j=0}^{m}\left(1 + 10^{pK_{a,j}^{bound} - pH}\right)}{\prod_{j=0}^{m}\left(1 + 10^{pK_{a,j}^{free} - pH}\right)} \\
\Delta n_{LB,H} &= \sum_{j=0}^{m} \frac{10^{pK_{a,j}^{bound} - pH}}{1 + 10^{pK_{a,j}^{bound} - pH}} - \sum_{j=0}^{m} \frac{10^{pK_{a,j}^{free} - pH}}{1 + 10^{pK_{a,j}^{free} - pH}} \\
\Delta H_0 &= \Delta H_{int} + \sum_{j=0}^{m} \frac{10^{pK_{a,j}^{bound} - pH}}{1 + 10^{pK_{a,j}^{bound} - pH}} \Delta H_{a,j}^{bound} \\
&\quad - \sum_{j=0}^{m} \frac{10^{pK_{a,j}^{free} - pH}}{1 + 10^{pK_{a,j}^{free} - pH}} \Delta H_{a,j}^{free}
\end{aligned} \tag{30}$$

where ΔH_{int} is the pH-independent (completely deprotonated interacting species) ligand binding enthalpy and $\Delta H_{a,j}$ is the protonation enthalpy for a given proton binding site (which, similar to $pK_{a,j}$, may be different whether or not the ligand is bound). The proton binding subpolynomials $Z_{bound,H}$ and $Z_{free,H}$ have been conveniently factorized assuming that the set of proton binding sites behave independently, and the removal of the enthalpic contribution from the buffer indicated in Eq. 29 has previously been applied. These are well-known relationships for the pH dependency of ligand binding parameters due to coupling of proton exchange at ionizable groups [13, 30].

Allostery exists beyond protein interactions, and similar phenomena can be found in other systems. In particular, the formation of pH-dependent non-canonical base pairs in DNA and RNA coupled to changes in pK_a's is another appropriate example of interaction coupled to proton exchange, similar to the interaction of the inhibitors with the HIV-1 protease [31].

Example 3: NQO1 shows homotropic FAD-binding cooperativity

NQO1 NAD(P)H quinone dehydrogenase 1 is an FAD-binding homodimeric protein responsible for the reduction of quinones and intervening in essential cellular detoxification processes and activation of antitumor quinone-

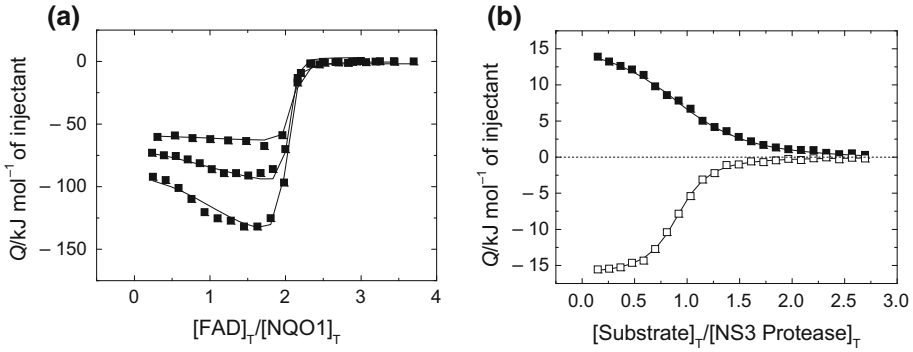

Fig. 5 **a** Calorimetric titrations for NQO1 interacting with FAD at different temperatures. Increasing the temperature led to a more pronounced enthalpically favored cooperativity effect. Applying a global analysis for a homotropic protein with two ligand binding sites together with the van't Hoff equation for the intrinsic and cooperative binding parameters allowed estimating the intrinsic binding parameters ($\beta_1 = 1.8{\cdot}10^8$ M^{-1}, $\Delta H_1 = -93$ kJ mol^{-1}, $\Delta C_{P1} = -3.3$ kJ K^{-1} mol^{-1}) and the cooperative binding parameters ($\alpha_2 = 0.53$, $\Delta h_2 = -50$ kJ mol^{-1}, $\Delta c_{P2} = -4.6$ kJ K^{-1} mol^{-1}) at 25 °C [34]. **b** Calorimetric titrations for hepatitis *C* virus NS3 protease interacting with its substrate in the absence (closed squares) and the presence (open squares) of the viral NS4A cofactor (at 200 μM concentration of NS4A, with $\beta_{01} = 10^5$ M^{-1}, which represents an almost saturating concentration) [38]. The inactive single-point mutant S139A of the protease was employed. Substrate titrated into the protease provided the binding parameters: $\beta_{10} = 8.1{\cdot}10^5$ M^{-1}, $\Delta H_{10} = 16.3$ kJ mol^{-1}), and the apparent binding parameters: $\beta_{10}^{app} = 4.2{\cdot}10^6$ M^{-1}, $\Delta H_{10}^{app} = -16.2$ kJ mol^{-1}). Then, the cooperative interaction parameters can be calculated: $\alpha_{11} = 5.2$ and $\Delta h_{11} = -32.5$ kJ mol^{-1}, according to Eq. 37 [38]. With no approximation (Eq. 36), a value of 5.4 is estimated for α_{11}

related prodrugs [32]. Deficiency in NQO1 activity results in decreased p53 stability, as well as chemoresistance due to inefficient prodrug activation. NQO1-FAD interaction is an excellent system to study homotropic cooperativity, because NQO1 binds two FAD molecules per dimer in a cooperative fashion [33].

A global analysis of calorimetric titrations (Fig. 5a) at different temperatures was performed applying a homotropy model for two binding sites ($n = 2$) [7, 8, 34]:

$$Z = 1 + \beta_1[A] + \beta_2[A]^2 \tag{31}$$

where the constants β's already contain implicitly the conformational heterogeneity in the protein (Eq. 8). According to Eqs. 4 and 49, the binding polynomial can be written in terms of the overall constant β_1 (or the site-specific association constant K) and the homotropic cooperativity constant α_2:

$$Z = 1 + \beta_1[A] + \frac{1}{4}\beta_1^2\alpha_2[A]^2 = 1 + 2K[A] + K^2\alpha_2[A]^2 \tag{32}$$

The influence of the temperature was implemented considering the extended van't Hoff equation with nonzero binding heat capacity in order to estimate the intrinsic FAD-binding parameters and the cooperative FAD-binding parameters (Fig. 5a). The cooperative behavior of FAD binding is not apparent at all temperatures, because of the temperature dependency of the cooperativity binding parameters. Thus, the requirement for performing titrations at different temperatures in order to confirm whether or not ligand binding to a given protein is cooperative cannot be overemphasized. From those experiments, it was concluded that the second FAD molecule binds to the dimer with half the binding affinity of the first molecule ($\alpha_2 = 0.53$), and this cooperative effect is dominated by a favorable enthalpic contribution of -50 kJ mol^{-1}, accompanied by an unfavorable entropic contribution of 52 kJ mol^{-1} [34].

Communication of biochemical signals within multimeric allosteric proteins still remains poorly understood, even for dimeric systems such as NQO1. Homodimeric proteins represent model systems for observing conformational and dynamic processes interconnecting active sites. Combined complementary experimental techniques can be used to assess binding and cooperativity energetics, as well as local and global structural changes occurring in the protein [35].

Example 4: Hepatitis C virus NS3 protease shows heterotropic substrate and NS4A cofactor binding cooperativity

The life cycle of the hepatitis *C* virus in infected cells requires the expression of a polyprotein that must be processed by host and viral proteases [36, 37]. NS3 protease is one of those two viral proteases and a main therapeutic target against hepatitis C virus. NS3 protease is a zinc-dependent enzyme which requires the binding of an additional viral cofactor, NS4A, for proper configuration of the catalytic triad in the substrate binding site. The interplay between substrate and cofactor was studied by ITC considering a simple heterotropic model for two ligands binding to a protein ($n = 1$, $m = 1$) [7, 38]:

$$Z = 1 + \beta_{10}[A] + \beta_{01}[B] + \beta_{11}[A][B] \tag{33}$$

that can be written in terms of the heterotropic interaction constant α_{11}:

$$Z = 1 + \beta_{10}[A] + \beta_{01}[B] + \beta_{10}\beta_{01}\alpha_{11}[A][B] \tag{34}$$

Instead of solving the ternary equilibrium (Eq. 13) [39, 40], the binding polynomial can be renormalized on the basis of ligand B (Eq. 15):

$$Z = 1 + \beta_{10}\frac{1 + \beta_{01}\alpha_{11}[B]}{1 + \beta_{01}[B]}[A] = 1 + \beta_{10}^{app}[A] \tag{35}$$

from which the following relationships can be obtained (see Eq. 61):

$$\begin{aligned} \beta_{10}^{app} &= \beta_{10}\frac{1 + \beta_{01}\alpha_{11}[B]}{1 + \beta_{01}[B]} \\ \Delta H_{10}^{app} &= \Delta H_{10} - \frac{\beta_{01}[B]}{1 + \beta_{01}[B]}\Delta H_{01} \\ &\quad + \frac{\beta_{01}\alpha_{11}[B]}{1 + \beta_{01}\alpha_{11}[B]}(\Delta H_{01} + \Delta h_{11}) \end{aligned} \tag{36}$$

where Δh_{11} is the binding cooperativity enthalpy.

If ligand B can be employed at a saturating concentration, the apparent binding parameters for ligand A are simplified to:

$$\begin{aligned} \beta_{10}^{app} &\approx \beta_{10}\alpha_{11} \\ \Delta H_{10}^{app} &\approx H_{10} + \Delta h_{11} \end{aligned} \tag{37}$$

and then, the cooperativity parameters can be readily estimated through Eq. 37 by just performing two titrations and analyzing them as simple binary titrations: One titration consists of injecting ligand A into protein (binary titration) and provides β_{10} and ΔH_{10}, and the other one consists of injecting ligand A into protein mixed with ligand B at saturating concentration (ternary titration) and provides β_{10}^{app} and ΔH_{10}^{app}. Otherwise, there are two alternatives: (1) obtain the intrinsic binding parameters for each ligand through binary titrations (β_{10}, β_{01}, ΔH_{10} and ΔH_{01}), and then, perform a ternary titration and solve the exact ternary equilibrium in order to account explicitly for the interplay between both ligands and obtain α_{11} and Δh_{11} [39, 40]; or (2) perform several ternary titrations under different ligand B concentrations, analyze them as binary titrations, obtain β_{10}^{app} and ΔH_{10}^{app} at several ligand B concentrations, and use Eqs. 36 in order to estimate the intrinsic binding parameters (β_{10}, β_{01}, ΔH_{10} and ΔH_{01}), and the cooperative binding parameters (α_{11} and Δh_{11}) by nonlinear regression analysis [40, 41]. The problem in this last procedure is that at low/moderate ligand B concentration the concentration of ligand B is not constant through the calorimetric titration, and if the affinity of ligand B is high, subsaturating concentrations of ligand B may result in biphasic binding isotherms. From the previous discussion, the differences between β_{10}, β_{10}^{app} and $\beta_{10}\alpha_{11}$ are obvious: β_{10}^{app} is an apparent association constant for ligand A dependent on concentration and binding affinity of ligand B. β_{10}^{app} has two limiting vales: (1) β_{10}, the intrinsic association constant for ligand A in the absence of ligand B, and (2) $\beta_{10}\alpha_{11}$, the value for β_{10}^{app} at very high concentration of ligand B.

According to Eq. 37, performing just two titrations (substrate as ligand A into enzyme and substrate into enzyme saturated with NS4A cofactor as ligand B), it was possible to obtain the binding parameters for the substrate binding to the enzyme: $\beta_{10} = 8.1{\cdot}10^5$ M^{-1}, $\Delta H_{10} = 16.3$ kJ mol^{-1}, as well as the apparent binding parameters for the substrate binding to the protein in the presence of saturating cofactor concentration: $\beta_{10}^{app} = 4.2{\cdot}10^6$ M^{-1}, $\Delta H_{10}^{app} = -16.2$ kJ mol^{-1} (Fig. 5b) [38]. Then, the cooperative interaction parameters, $\alpha_{11} = 5.2$ and $\Delta h_{11} = -32.5$ kJ mol^{-1}, could be calculated using Eq. 37, without the need for determining the intrinsic binding parameters for the NS4A cofactor (β_{01} and ΔH_{01}). Substrate and NS4A cofactor binding show positive heterotropic cooperativity: The binding of any of the two ligands increases the binding affinity of the other ligand by a fivefold factor.

Example 5: Interaction of nucleotides with F_1-ATPase subunits is modulated by magnesium through an heterotropic cooperative fashion

The F-ATPase is part of the mitochondrial machinery responsible for synthesizing ATP from the chemical energy stored as an electrochemical gradient of protons generated through electron transfer processes [42]. The F_1 domain of the ATPase is oriented toward the mitochondrial matrix and is able to synthesize ATP from ADP, while the F_0 domain is embedded in the mitochondrial inner membrane and is in charge of coupling the energetically favorable channeling of protons from the intermembrane space to the matrix. Among other elements, F_1 domain contains three alpha and three beta subunits conforming a heterohexamer. Each subunit is able to interact with ADP and ATP. Because nucleotides are very often complexed with magnesium, in order to understand the global ATP synthesis process, it was important to determine: (1) the ability of those subunits for discriminating both nucleotides and (2) the influence of magnesium in the nucleotide recognition.

For that purpose, the interaction of ATP and ADP with alpha and beta subunits was measured by ITC in the absence and the presence of magnesium [43, 44]. The binary experiments consisting in titrating nucleotides into protein subunits do not pose any problem, but in the ternary

experiments it will be difficult to extract meaningful information unless we deal with the underlying complexity: Nucleotides can bind magnesium, and there will be different species populations (free nucleotide, nucleotide with one magnesium ion bound and nucleotide with two magnesium ions bound in the case of ATP); at the same time, protein subunits may interact with magnesium-free and magnesium-bound nucleotides.

The interplay between the three elements can be best studied if we center the system on the nucleotide molecule, which is able to interact with magnesium and protein subunits. Thus, magnesium (ligand B) and protein subunit (ligand A) play the role of ligands for the nucleotide. These ligands show homotropic cooperativity (magnesium binding to nucleotide) and heterotropic cooperativity. Therefore, this is an example of homotropy and heterotropy coupling. The binding polynomial for the system is ($n = 1$, $m = 2$):

$$Z = 1 + \beta_{10}[A] + \beta_{01}[B] + \beta_{02}[B]^2 + \beta_{11}[A][B] \tag{38}$$

with $\beta_{02} = 0$ in the case of ADP. This expression can be written in terms of the homotropic and heterotropic interaction constants α_2^B and α_{11} (see Eqs. 4 and 49):

$$Z = 1 + \beta_{10}[A] + \beta_{01}[B] + \frac{1}{4}\beta_{01}^2\alpha_2^{\mathrm{B}}[B]^2 + \beta_{10}\beta_{01}\alpha_{11}[A][B] \tag{39}$$

Renormalization of the binding polynomial for simplifying the system does not offer much benefit, and the ternary equilibrium must be solved (Eq. 13). Therefore, a set of experiments was performed: (1) magnesium titrated into nucleotide (for estimating β_{01} and ΔH_{11}, and β_{02} and ΔH_{02}, or α_2^{B} and Δh_2^{B}); (2) nucleotide titrated into protein subunit (for estimating β_{10} and ΔH_{10}); and (3) nucleotide titrated into protein subunit in the presence of magnesium (for estimating α_{11} and Δh_{11}) [43, 44]. From those experiments, it was found that: (1) beta subunit binds Mg^{+2}:ATP and Mg^{+2}:ADP with similar affinity, while alpha subunit binds Mg^{+2}:ATP with higher affinity; (2) there is negative homotropic cooperativity for ATP interacting with Mg^{+2} ($\alpha_2^{\mathrm{B}} = 0.01$); (3) there is positive heterotropic cooperativity for ATP and Mg^{+2} binding to beta and alpha subunits ($\alpha_{11} = 8$ and 300, respectively); and (4) there is negligible heterotropic cooperativity for ADP and Mg^{+2} binding to beta and alpha subunits (α_{11} close to 1).

Although this formalism is appropriate, it is interesting to note that, contrary to FAD binding to homodimeric NQO1, magnesium binding to ATP could not be considered as a system with two identical binding sites with homotropic cooperativity, but two nonidentical binding sites with intrinsic site-specific association constants K_1 and K_2 (with $K_1 > K_2$). In that case, the site-specific association constants for magnesium binding to ATP are related to the overall association constants by:

$$\begin{aligned} \beta_{01} &= K_1 + K_2 \\ \beta_{02} &= K_1 K_2 \end{aligned} \tag{40}$$

and

$$\begin{aligned} K_1 &= \frac{1}{2}\beta_{01}\left(1 + \sqrt{1 - \alpha_2^{\mathrm{B}}}\right) \\ K_2 &= \frac{1}{2}\beta_{01}\left(1 - \sqrt{1 - \alpha_2^{\mathrm{B}}}\right) \end{aligned} \tag{41}$$

from which

$$\alpha_2^{\mathrm{B}} = \frac{4K_1K_2}{(K_1 + K_2)^2} \tag{42}$$

If $\alpha_2^{\mathrm{B}} = 1$, then $K_2 = K_1$ and both sites are identical and there is no homotropic effect; if $\alpha_2^{\mathrm{B}} = 0$, then $K_2 = 0$ and both sites are reciprocally excluding each other and exhibit maximal negative homotropic cooperativity. For small values of α_2^{B} (i.e., $K_2 \ll K_1$), which is the case for ATP/magnesium:

$$\begin{aligned} K_1 &\approx \beta_{01}\left(1 - \frac{\alpha_2^{\mathrm{B}}}{4}\right) \\ K_2 &\approx \beta_{01}\frac{\alpha_2^{\mathrm{B}}}{4} \\ \frac{K_2}{K_1} &\approx \frac{\alpha_2^{\mathrm{B}}}{4} \end{aligned} \tag{43}$$

Similar control and regulatory mechanisms exerted by metal ions can be found in other systems. In particular, RNA interaction with magnesium is another nice example of allosteric control of conformation by ligand interaction, resulting in considerable structural rearrangements in RNA, which will influence subsequent binding of other ligands through cooperative heterotropic interactions [45].

Final remarks

In biological interactions, both thermodynamics and kinetics govern the populations of the different possible conformational states, ligand complexes and their interconversions. In fact, protein conformational dynamics can dictate binding affinity [46], which may modulate further interactions. Reciprocally, allosteric control of the conformational landscape may not only alter the predominant conformational states by stabilizing and populating certain preferential Gibbs energy basin locations in the conformational landscape and resulting in conformational transitions, but it also modulates the width of those Gibbs energy basins which dictates the dynamic properties of the

conformational states and the rates of the conformational transitions [47, 48]. The reduced amount of accumulated knowledge on the dynamics of allosteric transitions in proteins is likely due to the small size of structural changes in the protein elicited by allosteric effectors and the challenges in the design of appropriate experiments directed at observing those allosteric transitions [49].

The binding polynomial is a general representation of all protein species in equilibrium, which, though a limited representation that overlooks protein kinetics and dynamics, is a useful steady-state representation that describes reasonably well key aspects of the system. The main benefit from using the binding polynomial formalism is twofold. First, it provides a general, systematic, versatile framework for the description of the chemical equilibria in biological interactions, even for allosteric or polysteric systems. And second, it provides tools (e.g., linkage relationships and Wyman representation) that can be employed in a straightforward way to extract valuable information about those biological interactions, without the need to develop system-dependent ad hoc procedures.

Allosteric interactions are physiologically important for controlling and regulating protein function and protein-dependent signaling networks. Therefore, distortion of allosteric interactions, caused directly by protein mutations or indirectly by inappropriate provision of allosteric effectors, may constitute the molecular basis of a disease [50, 51]. On the other hand, allosteric effectors represent an important set of potential drugs intended for innovative therapies [52]. Allosteric drugs may exhibit strategic advantages; in particular, allosteric ligands do not have to compete with natural ligands for binding to the orthosteric site in the protein target, and they may show better target specificity and selectivity profile provided that allosteric sites seem to be less conserved than orthosteric sites [50]. Allosteric drugs may be even more important in the case of targeting protein–protein interactions, fundamental elements in a wide range of biological processes, which, due to their large, shallow and featureless binding interfaces, are quite challenging for small molecule drug design [53].

Allostery has been thought to rely on well-defined intramolecular pathways able to communicate and transmit structural and dynamical perturbations between distant locations within the protein molecule. However, a wider interpretation and description of allostery in terms of the energetics of conformational changes and allosteric interactions has made possible to explain observations in scenarios apparently lacking site-to-site coupling and intermolecular pathways: allosteric phenomena in the absence of structural distortions and the ability of some effectors to act as allosteric agonists or antagonists depending on the circumstances [54].

Allosteric interactions are important for all proteins. However, because of the remarkable structural plasticity of intrinsically disordered proteins and their ability to adapt to multiple environments exemplified by their capability to interact with numerous biological partners, allosteric interactions may be even more important among this group of proteins [55–57]. In fact, allostery within or mediated by intrinsically disordered proteins ensures robust and efficient biochemical signal integration and transduction through mechanisms that would be unfavorable or even impossible for well-folded proteins [58, 59].

The MWC and KNF can be used to simplify the conformational landscape and reduce the complexity of the binding polynomial and the description of the cooperative protein system. While these two models are able to reproduce homotropic cooperative behavior, they show significant differences: (1) MWC cannot be applied for negative ligand binding cooperativity; (2) MWC only involves two conformational states linked by a global concerted conformational change in the protein, while KNF involves a sequence of local conformational changes, with as many conformational states as the number of ligand binding sites; (3) if the number of binding sites is larger than 3, KNF requires more parameters than MWC; and (4) because of the global concerted structural and functional change, MWC is able to explain a simultaneous dual activating/inhibiting role for the same ligand [60], while the gradual, sequential structural and functional change in KNF is only able to explain an activating or inhibiting role for a given ligand.

Finally, a protein with a single binding site for ligand A cannot exhibit a biphasic titration (i.e., a titration for which the isotherm shows more than one potential inflection point). By particularizing Eqs. 8 and 15 for $n = 1$, it is obvious that the protein must exhibit a single apparent binding association and, therefore, a single apparent binding enthalpy. From Eq. 8, the apparent binding constant is the population-weighted average binding constant over the ensemble with all possible conformational estates. Non-binding conformational states contribute by reducing the effective apparent binding constant; however, if they are in equilibrium within the global ensemble, they do not reduce the fraction of binding-competent protein because of their interconversion with binding states (unless there are remarkable kinetic barriers). And from Eq. 15, the apparent binding constant is the normalized binding constant considering the binding subpolynomials for ligand B, with the subensemble of ligand A-free states as a reference. Consequently, if a non-monophasic binding isotherm is observed for ligand A, it is possible that: (1) there is more than one binding site for ligand A (with or without cooperativity); (2) there is no equilibrium between some protein conformational exhibiting different affinities for ligand A;

(3) there is no equilibrium between some ligand *B*-bound states exhibiting different affinities for ligand *A*; or (4) ligand *B* shows high affinity and allosteric coupling with ligand *A* and is present at a subsaturating concentration. In other words, in general, conformational changes or secondary ligands (un)binding cannot be invoked to explain non-monophasic titrations.

It is important to remind that, in principle, there is a huge number of possible conformational states and a huge number of possible secondary ligands for a given protein, all of them a priori unknown or irrelevant to the experimenter, and they can be implicitly considered and hidden within the apparent binding constants when a simplified or renormalized form of the binding polynomial is employed. The experimental strategy usually starts with the simplest model and binding polynomial, and as the number of factors (temperature, pH, co-solutes and additional ligands) entering into play increases and more information on the interaction is gathered, the binding polynomial may be conveniently expanded/simplified. Thus, conformational changes or secondary ligand binding are not explicitly reflected in the calorimetric isotherms, but through the dependency of the apparent binding parameters on the environmental variables (temperature, pH, ionic strength, co-solute concentration, etc.).

Acknowledgements This work was supported by Miguel Servet Program from Instituto de Salud Carlos III (CPII13/00017 to OA); Fondo de Investigaciones Sanitarias from Instituto de Salud Carlos III, and European Union (ERDF/ESF, 'Investing in your future') (PI15/00663 and PI18/00349 to OA); Spanish Ministry of Economy and Competitiveness (BFU2016-78232-P to AVC); Diputación General de Aragón (Protein Targets and Bioactive Compounds Group E45_17R to AVC, and Digestive Pathology Group B25_17R to OA); and Centro de Investigación Biomédica en Red en Enfermedades Hepáticas y Digestivas (CIBERehd).

Compliance with ethical standards

Conflict of interest The authors declare that they have no conflict of interest.

Appendix

The overall association constants β_i can be expressed as a function of β_1

It can be demonstrated that the overall stoichiometric association constant β_{si} for the formation of complex P_sA_i can be expressed as a function of the total number of binding sites, n, the number of ligand A molecules bound per macromolecule, i, the intrinsic site-specific association constant for ligand A, β_{s1} (that is, the overall stoichiometric association constant for the formation of complex P_sA), and the cooperativity constant accounting for homotropic cooperativity effects for ligand A binding, α_{si}:

$$\beta_{si} = \binom{n}{i} n^{-i} \beta_{s1}^{i} \alpha_{si} \tag{44}$$

If a protein conformational state P has n identical and independent binding sites for ligand A, the binding polynomial factorizes into identical terms, each one representing one of the ligand binding sites as a subsystem:

$$Z = \sum_{i=0}^{n} \beta_i [A]^i = (1 + K[A])^n \tag{45}$$

where K is the intrinsic site-specific association constant for each of the ligand binding sites. From that expression, it is obvious that:

$$\beta_i = \binom{n}{i} K^i \tag{46}$$

with:

$$\beta_1 = nK \tag{47}$$

and from that:

$$\beta_i = \binom{n}{i} n^{-i} \beta_1^i \tag{48}$$

Then, potential homotropic cooperative effects can be accounted for by introducing an additional factor α_i, with $\alpha_1 = 1$, because there is no homotropic effect for the first bound ligand:

$$\beta_i = \binom{n}{i} n^{-i} \beta_1^i \alpha_i \tag{49}$$

This expression is completely general and it can be applied to any situation (i.e., identical or nonidentical binding sites, cooperative or non-cooperative sites) by decomposing β_1 and α_i into additional factors [8]. Such decomposition will help in reducing the number of binding parameters required in the model [61].

From Eq. (46), the binding polynomial can be factorized into identical terms if, for all i's, it is fulfilled that [1]:

$$\frac{\frac{\beta_i}{\binom{n}{i}}}{\left(\frac{\beta_{i-1}}{\binom{n}{i-1}}\right)^{i/i-1}} = 1 \tag{50}$$

And it can be factorized into nonidentical terms if, for all i's, it is fulfilled that [1]:

$$\frac{\frac{\beta_i}{\binom{n}{i}}}{\left(\frac{\beta_{i-1}}{\binom{n}{i-1}}\right)^{i/i-1}} < 1 \tag{51}$$

Therefore, the ligand binding sites are identical and independent if:

$$\frac{\alpha_i}{(\alpha_{i-1})^{i/i-1}} = 1 \tag{52}$$

and the ligand binding sites are nonidentical and independent if:

$$\frac{\alpha_i}{(\alpha_{i-1})^{i/i-1}} < 1 \tag{53}$$

Thus, the independent and identical nature of the ligand binding sites can be judged by comparing the overall association constants (β's) or the homotropic cooperativity parameters (α's).

The extent of the heterotropic effect between ligand *A* and ligand *B* is fully reciprocal

The heterotropic effect between two ligands is fully reciprocal or symmetric. Because of the energy conservation principle, if ligand B modifies the intrinsic affinity for ligand A by a factor α_{ij}, then ligand A causes the same effect on ligand B. The constant β_{ij} can be split into two factors: $\beta_{ij} = \beta_{i0}\beta_{j/i}$, where β_{i0} is the overall association constant for $P + A_i \leftrightarrow PA_i$ and $\beta_{j/i}$ is the overall association constant for $PA_i + B_j \leftrightarrow PA_iB_j$. Alternatively, β_{ij} can be split into two factors: $\beta_{ij} = \beta_{0j}\beta_{i/j}$, where β_{oj} is the overall association constant for $P + B_j \leftrightarrow PB_j$ and $\beta_{i/j}$ is the overall association constant for $PB_j + A_i \leftrightarrow PA_iB_j$. Furthermore, the constants $\beta_{j/i}$ and $\beta_{i/j}$ can be factorized as: $\beta_{j/i} = \beta_{0j}\alpha_{ij}$ and $\beta_{i/j} = \beta_{i0}\alpha_{ij}$.

The maximal allosteric effect occurs at concentrations around the dissociation constant of the ligand

From Eq. 20, if, for the sake of simplicity, only a single binding site for ligand B is considered:

$$\frac{\partial \ln \gamma_s^{app}}{\partial \ln[B]} = \Delta n_{LB,s,B} = \frac{\beta_s[B]}{1+\beta_s[B]} - \frac{\beta_0[B]}{1+\beta_0[B]} \tag{54}$$

$\Delta n_{LB,s,B}$ will be zero for zero and infinite ligand B concentration, and for $\beta_s = \beta_0$. Deriving with respect to ligand B concentration:

$$\frac{\partial \Delta n_{LB,s,B}}{\partial \ln[B]} = \frac{\beta_s[B]}{(1+\beta_s[B])^2} - \frac{\beta_0[B]}{(1+\beta_0[B])^2} \tag{55}$$

and a maximal value for $\Delta n_{LB,s,B}$ will be achieved when:

$$\beta_s - \beta_0 - \beta_s\beta_0(\beta_s - \beta_0)[B]^2 = 0 \tag{56}$$

whose solutions are: (1) $\beta_s = \beta_0$ and any value of $[B]$ (trivial case); or (2) $\beta_s \neq \beta_0$ and $[B] = (\beta_s\beta_0)^{-1/2}$, the inverse of the geometric mean of the overall association constants, which is the concentration of ligand B for a maximal allosteric effect on the apparent conformational constant γ_s^{app} for P_s.

The maximal heterotropic effect occurs at concentrations around the dissociation constant of the secondary ligand

From Eq. 25, if there are several ($i = 1 \ldots n$) binding sites for ligand A and, for the sake of simplicity, a single binding site for ligand B:

$$\frac{\partial \ln \beta_i^{app}}{\partial \ln[B]} = \Delta n_{LB,i,B} = \frac{\beta_{01}\alpha_{i1}[B]}{1+\beta_{01}\alpha_{i1}[B]} - \frac{\beta_{01}[B]}{1+\beta_{01}[B]} \tag{57}$$

$\Delta n_{LB,i,B}$ will be zero for zero and infinite ligand B concentration, and for $\alpha_{i1} = 1$. Deriving with respect to ligand B concentration:

$$\frac{\partial \Delta n_{LB,i,B}}{\partial \ln[B]} = \frac{\beta_{01}\alpha_{i1}[B]}{(1+\beta_{01}\alpha_{i1}[B])^2} - \frac{\beta_{01}[B]}{(1+\beta_{01}[B])^2} \tag{58}$$

and a maximal value for $\Delta n_{LB,B}$ will be achieved when:

$$\alpha_{i1} - 1 - \beta_{01}^2\alpha_{i1}(\alpha_{i1} - 1)[B] = 0 \tag{59}$$

whose solutions are: (1) $\alpha_{i1} = 1$ and any value of β_{01} and $[B]$ (trivial case); or (2) $\alpha_{i1} \neq 1$ and $[B] = \beta_{01}^{-1}\alpha_{i1}^{-1/2}$, which is the concentration of ligand B for a maximal heterotropic effect on the apparent overall association constant β_i^{app} for PA_i.

Enthalpy changes associated with equilibrium constants are calculated by applying the van't Hoff equation

Every equilibrium constants has an associated enthalpy change (besides changes in other thermodynamic potentials). The corresponding enthalpy change can be calculated by applying the van't Hoff equation:

$$\Delta H = RT^2 \frac{\partial \ln K_{eq}}{\partial T} \tag{60}$$

From that, if a given equilibrium constant is a function of other equilibrium constants, then, the corresponding enthalpy can be calculated by applying Eq. 53:

$$K_{eq} = f\left(\left\{K_{eq,r}\right\}\right)$$
$$\Delta H = RT^2 \frac{\partial \ln K_{eq}}{\partial T} = RT^2 \frac{\partial \ln f\left(\left\{K_{eq,r}\right\}, \left\{\Delta H_r\right\}\right)}{\partial T} \quad (61)$$

References

1. Wyman J, Gill SJ. Binding and linkage: functional chemistry of biological macromolecules. Mill Valley: University Science Books; 1990.
2. Schellman JA. Macromolecular binding. Biopolymers. 1975;14:999–1018.
3. Wyman J. The binding potential, a neglected linkage concept. J Mol Biol. 1965;11:631–44.
4. Wyman J. Linked functions and reciprocal effects in hemoglobin—A second look. Adv Protein Chem. 1964;19:223–86.
5. Velazquez-Campoy A. Geometric features of the Wiseman isotherm in isothermal titration calorimetry. J Thermal Anal Calorim. 2015;122:1477–83.
6. Velazquez-Campoy A. Allostery and cooperative interactions in proteins assessed by isothermal titration calorimetry. In: Bastos M, editor. Biocalorimetry—foundations and contemporary approaches. Boca Raton: CRC Press; 2016. p. 223–46.
7. Vega S, Abian A, Velazquez-Campoy A. A unified framework based on the binding polynomial for characterizing biological systems by isothermal titration calorimetry. Methods. 2015;76:99–115.
8. Freire E, Schön A, Velazquez-Campoy A. Isothermal titration calorimetry: general formalism using binding polynomials. Methods Enzymol. 2009;455:127–55.
9. Bohr C, Hasselbalch K, Krogh A. Ueber einen in biologischer beziehung wichtigen einfluss, den die kohlensäurespannung des blutes auf dessen sauerstoffbindung übt. Skand Archiv Physiol (Acta Physiol). 1904;16:402–12.
10. Monod J, Wyman J, Changeux JP. On the nature of allosteric transitions a plausible model. J Mol Biol. 1965;12:88–118.
11. Monod J, Changeux JP, Jacob F. Allosteric proteins and cellular control systems. J Mol Biol. 1963;6:306–29.
12. Gunasekaran K, Ma B, Nussinov R. ls allostery an intrinsic property of all dynamic proteins? Proteins. 2004;57:433–43.
13. Eftink M, Biltonen RL. Thermodynamics of interacting biological systems. Beezer AE, Biological calorimetry". London: Academic Press; 1980. p. 343–412.
14. Courter JR, Madani N, Sodroski J, Schön A, Freire E, Kwong PD, Hendrickson WA, Chaiken IM, LaLonde JM, Smith AB 3rd. Structure-based design, synthesis and validation of CD4-mimetic small molecule inhibitors of HIV-1 entry: conversion of a viral entry agonist to an antagonist. Acc Chem Res. 2014;47:1228–37.
15. Williams R, Holyoak T, McDonald G, Gui C, Fenton AW. Differentiating a ligand's chemical requirements for allosteric interactions from those for protein binding. Phenylalanine inhibition of pyruvate kinase. Biochemistry. 2006;45:5421–9.
16. Jobichen C, Fernandis AZ, Velazquez-Campoy A, Leung KY, Mok YK, Wenk MR, Sivaraman J. Identification and characterization of the lipid-binding property of GrlR, a locus of enterocyte effacement regulator. Biochem J. 2009;13(420):191–9.
17. Rodriguez-Cardenas A, Rojas AL, Conde-Gimenez M, Velazquez-Campoy A, Hurtado-Guerrero R, Sancho J. Streptococcus pneumoniae TIGR4 flavodoxin: structural and biophysical characterization of a novel drug target. PLoS ONE. 2016;11:e0161020.
18. Cremades N, Velazquez-Campoy A, Freire E, Sancho J. The flavodoxin from Helicobacter pylori: structural determinants of thermostability and FMN cofactor binding. Biochemistry. 2008;47:627–39.
19. Irun MP, Garcia-Mira MM, Sanchez-Ruiz JM, Sancho J. Native hydrogen bonds in a molten globule: the apoflavodoxin thermal intermediate. J Mol Biol. 2001;306:877–88.
20. Wyman J. Heme proteins. Adv Protein Chem. 1948;4:407–531.
21. Wyman J. Allosteric linkage. J Am Chem Soc. 1967;89:2202–18.
22. Koshland DE Jr, Nemethy G, Filmer D. Comparison of experimental binding data and theoretical models in proteins containing subunits. Biochemistry. 1966;5:365–85.
23. Di Cera E, Gill SJ, Wyman J. Binding capacity: cooperativity and buffering in biopolymers. Proc Natl Acad Sci USA. 1988;85:449–52.
24. Ji Y, Postis VL, Wang Y, Bartlam M, Goldman A. Transport mechanism of a glutamate transporter homologue GltPh. Biochem Soc Trans. 2016;44:898–904.
25. Groeneveld M, Slotboom DJ. Na(+): aspartate coupling stoichiometry in the glutamate transporter homologue Glt(Ph). Biochemistry. 2010;49:3511–3.
26. Boudker O, SeCheol O. Isothermal titration calorimetry of ion-coupled membrane transporters. Methods. 2015;76:171–82.
27. Kohl NE, Emini EA, Schleif WA, Davis LJ, Heimbach JC, Dixon RA, Scolnick EM, Sigal IS. Active human immunodeficiency virus protease is required for viral infectivity. Proc Natl Acad Sci USA. 1988;85:4686–90.
28. Brik A, Wong C-H. HIV-1 protease: mechanism and drug discovery. Org Biomol Chem. 2003;1:5–14.
29. Velazquez-Campoy A, Luque I, Todd MJ, Milutinovich M, Kiso Y, Freire E. Thermodynamic dissection of the binding energetics of KNI-272, a potent HIV-1 protease inhibitor. Protein Sci. 2000;9:1801–9.
30. Baker BM, Murphy KP. Evaluation of linked protonation effects in protein binding reactions using isothermal titration calorimetry. Biophys J. 1996;71:2049–55.
31. Krishnamurthy R. Role of pKa of nucleobases in the origins of chemical evolution. Acc Chem Res. 2012;45:2035–44.
32. Ross D, Siegel D. Functions of NQO1 in cellular protection and CoQ10 metabolism and its potential role as a redox sensitive molecular switch. Front Physiol. 2017;8:595.
33. Pey AL, Megarity CF, Timson DJ. FAD binding overcomes defects in activity and stability displayed by cancer-associated variants of human NQO1. Biochim Biophys Acta—Mol Basis Dis. 2014;1842:2163–73.
34. Claveria-Gimeno R, Velazquez-Campoy A, Pey AL. Thermodynamics of cooperative binding of FAD to human NQO1: implications to understanding cofactor-dependent function and stability of the flavoproteome. Arch Biochem Biophys. 2017;636:17–27.
35. Lee AL, Sapienza PJ. Thermodynamic and NMR assessment of ligand cooperativity and intersubunit communication in symmetric dimers: application to thymidylate synthase. Front Mol Biosci. 2018;5:47.
36. Tomei L, Failla C, Santolini E, De Francesco R, La Monica N. NS3 is a serine protease required for processing of hepatitis C virus polyprotein. J Virol. 1993;67:4017–26.
37. Kwong AD, Kim JL, Rao G, Lipovsek D, Raybuck SA. Hepatitis C virus NS3/4A protease. Antivir Res. 1998;40:1–18.
38. Martinez-Julvez M, Abian O, Vega S, Medina M, Velazquez-Campoy A. Studying the allosteric energy cycle by isothermal titration calorimetry. Methods Mol Biol. 2012;796:53–70.
39. Martinez-Julvez M, Medina M, Velazquez-Campoy A. Binding thermodynamics of ferredoxin:NADP + reductase: two different protein substrates and one energetics. Biophys J. 2009;96:4966–75.
40. Velazquez-Campoy A, Goñi G, Peregrina JR, Medina M. Exact analysis of heterotropic interactions in proteins: characterization

of cooperative ligand binding by isothermal titration calorimetry. Biophys J. 2006;91:1887–904.
41. Du W, Liu W-S, Payne DJ, Doyle ML. Synergistic inhibitor binding to Streptococcus pneumoniae 5-enolpyruvylshikimate-3-phosphate synthase with both monovalent cations and substrate. Biochemistry. 2000;39:10140–6.
42. Jonckheere AI, Smeitink JAM, Rodenburg RJT. Mitochondrial ATP synthase: architecture, function and pathology. J Inherit Metab Dis. 2012;35:211–25.
43. Pulido NO, Salcedo G, Perez-Hernandez G, Jose-Nuñez C, Velazquez-Campoy A, Garcia-Hernandez E. Energetic effects of magnesium in the recognition of adenosine nucleotides by the F(1)-ATPase beta subunit. Biochemistry. 2010;49:5258–68.
44. Salcedo G, Cano-Sanchez P, Tuena de Gomez-Puyou M, Velazquez-Campoy A, Garcia-Hernandez E. Isolated noncatalytic and catalytic subunits of F1-ATPase exhibit similar, albeit not identical, energetic strategies for recognizing adenosine nucleotides. Biochim Biophys Acta—Bioenerg. 2014;1837:44–50.
45. Peselis A, Gao A, Serganov A. Cooperativity, allostery and synergism in ligand binding to riboswitches. Biochimie. 2015;117:100–9.
46. Seo M-H, Park J, Kim E, Hohng S, Kim H-S. Protein conformational dynamics dictate the binding affinity for a ligand. Nat Commun. 2014;5:3724.
47. Guo J, Zhou H-X. Protein Allostery and conformational dynamics. Chem Rev. 2016;116:6503–15.
48. Riera TV, Zheng L, Josephine HR, Min D, Yang W, Hedstrom L. Allosteric activation via kinetic control: potassium accelerates a conformational change in IMP dehydrogenase. Biochemistry. 2011;50:8508–18.
49. Stock G, Hamm P. A non equilibrium approach to allosteric communication. Philos Trans R Soc Lond B Biol Sci. 2018;373:20170187.
50. Nussinov R, Tsai C-J. Allostery in disease and drug discovery. Cell. 2013;153:293–305.
51. Abdel-Magid AF. Allosteric modulators: an emerging concept in drug discovery. ACS Med Chem Lett. 2015;6:104–7.
52. Lu S, Ji M, Ni D, Zhang J. Discovery of hidden allosteric sites as novel targets for allosteric drug design. Drug Discov Today. 2018;23:359–65.
53. Ni D, Lu S, Zhang J. Emerging roles of allosteric modulators in the regulation of protein-protein interactions (PPIs): a new paradigm for PPI drug discovery. Med Res Rev. 2019. https://doi.org/10.1002/med.21585.
54. Hilser VJ, Wrabl JO, Motlagh HN. Structural and energetic basis of allostery. Annu Rev Biophys. 2012;41:585–609.
55. Li J, Hilser VJ. Assessing allostery in intrinsically disordered proteins with ensemble allosteric model. Methods Enzymol. 2018;611:531–57.
56. Zhang L, Li M, Liu Z. A comprehensive ensemble model for comparing the allosteric effect of ordered and disordered proteins. PLoS Comput Biol. 2018;14:e1006393.
57. Hilser VJ, Thompson EB. Intrinsic disorder as a mechanism to optimize allosteric coupling in proteins. Proc Natl Acad Sci USA. 2007;104:8311–5.
58. Berlow RB, Dyson HJ, Wright PE. Expanding the paradigm: intrinsically disordered proteins and allosteric regulation. J Mol Biol. 2018;430:2309–20.
59. Li J, White JT, Saavedra H, Wrabl JO, Motlagh HN, Liu K, Sowers J, Schroer TA, Thompson EB, Hilser VJ. Genetically tunable frustration controls allostery in an intrinsically disordered transcription factor. eLife. 2017;6:e30688.
60. Felix J, Weinhäupl K, Chipot C, Dehez F, Hessel A, Gauto DF, Morlot C, Abian O, Gutsche I, Velazquez-Campoy A, Schanda P, Fraga H. Mechanism of the allosteric activation of the ClpP protease machinery by substrates and active-site inhibitors. Sci Adv. 2019. https://doi.org/10.1101/578260.
61. Taneva SG, Bañuelos S, Falces J, Arregi I, Muga A, Konarev PV, Svergun DI, Velazquez-Campoy A, Urbaneja MA. A mechanism for histone chaperoning activity of nucleoplasmin: thermodynamic and structural models. J Mol Biol. 2009;393:448–63.